Response to Referee #1

We would like to thank Referee #1 for taking the time to review our manuscript and appreciate the useful comments/corrections.

Major comments:

Do the authors have a view on the possible fraction of peatland/forest fires relative to agricultural burning?

Whilst this is difficult to quantify exactly, there has been some work in this area and approximately ¾ of the fuel consumption is estimated to have occurred as peatland burning. For further details, please see Huijnen et al., (2016) which includes some of our co-authors from this work. In the Supplementary Information of that paper the authors report that "From our total emissions estimate of 692 Tg CO2 produced in Sept-Oct 2015 over the region, 79% (548 Tg) can be attributed to CO2 originating from areas with peatland, based on the GFEDv3.1 peatland map".

We have added a section in the text to discuss this as well as including the relevant reference.

"It is estimated that approximately ¾ of the fire activity over this time period was due to peatland burning (Huijnen et al., 2016)."

Added in reference to:

Huijnen, V. *et al.* Fire carbon emissions over maritime southeast Asia in 2015 largest since 1997. *Sci. Rep.* **6**, 26886; doi: 10.1038/srep26886 (2016).

Minor comments/typographical:

Various typographical corrections

All typographical corrections have been fixed as recommended.

Is July used to determine the degree of enhancement (relative to October) as this is defined as the first month of fire activity (Figure 1)?

Yes. We'll clarify that in the text to better explain.

"In order to quantify the extreme nature of the October 2015 observations and to account for the annual growth rate, we define the magnitude of the enhancement as the October-July difference for each year, with July typically signifying the start of the fire season in this region".

Include the source of the peatland dataset

Now cited:
Ritung S., Wahyunto, Nugroho K. *et al.* (2011) Peatland map of Indonesia. Office of Research and Development of Land Resources. http://www.litbang.pertanian.go.id/unker/one/600/. Ministry of Agriculture.

Response to Referee #2

We would like to thank Referee #2 for taking the time to review our manuscript and appreciate the useful comments/corrections.

Major comments:

I understand number of good in-situ data is limited, but discussion on rough estimation of horizontal and vertical distribution of the plume is helpful to understand the usefulness of large footprint (10km), point-based and, column averaged observations of GOSAT.

During the extreme fire activity observed, plumes ranged in scale from small, low, isolated plumes to huge plumes covering much of the landmass. We have attempted to capture the extent of this large scale behaviour by including Figure 4, showing the GOSAT Cloud and Aerosol Imager data over the region.

It should be noted that whilst the GOSAT data is a column quantity, the shortwave infrared measurements are most sensitive to the surface and lower atmosphere (unlike for example the thermal infrared IASI measurements which are mainly sensitive to the mid-troposphere). Also as the referee notes, the sampling pattern of GOSAT is not necessarily suited to making such point-source measurements and future satellites with imaging capabilities such as Sentinel-5 Precursor would be more suited to this. However, as this work focuses on attempting to quantify the large-scale behaviour of the entire region, we believe that, while challenging, we were successful in identifying GOSAT soundings dominated by the fire emissions.

Further analysis or discussion on correlation between GOSAT-retrieved XCH4/XCO2 and CO will be useful.

Whilst we acknowledge that being able to use co-located CO measurements along with the CH4 and CO2 would be extremely valuable and aid in calculating emission factors, there were several issues that prevented us from being confident in doing so.

Firstly, CO is not available from GOSAT. The best option would likely be to use the IASI CO product however, there are certain issues in doing so. Firstly, the IASI L2 CO data available from Eumetsat had an undocumented bug in the data product, with any retrieved integrated column CO values above 4.0e-3 kg/m^2 being flagged as “invalid”. Due to the huge extent of these Indonesian values, this upper limit is regularly exceeded and means that no quantitative comparison can be done against this IASI data (although it can still be used qualitatively as we have done). We have passed this information on to Eumetsat and believe that they are currently fixing this bug in their product. Secondly, however, IASI has very different vertical sensitivity to GOSAT which means even if we were able to confidently co-locate soundings (with different overpass times), the comparison would be complicated to interpret. Whilst these issues can be overcome (e.g. through the use of assimilation into a chemistry transport model), we felt that this was potentially better suited to a future study. It should also be noted that GOSAT-2 (scheduled for launch in 2018) will be capable of measuring co-located CH4, CO2 and CO simultaneously.

Minor Comments

All typographical changes/recommendations have been included.

For CO2 retrieval do the authors use both 1.6 and 2.0 micron bands or only 1.6 micron band, which is closer to the CH4 band?

We only use the 1.6um CO2 band. This is described in more detail in our previous publications (e.g. Parker et al., 2015) and already stated in the text.

"this proxy method utilises the fact that the majority of the influence of atmospheric scattering on the retrieved XCH4 can be negated through the co-retrieval of the spectrally close 1.6 µm CO2 band"

Description on CAI will help reader's understanding

We have added the following section to the text to provide more details.

"The second instrument is the Cloud and Aerosol Imager (TANSO-CAI), which provides multispectral imagery at 0.5 km resolution with bands at 0.38 µm, 0.67 µm, 0.87 µm and 1.6 µm. This allows additional cloud/aerosol information about the region of interest within which the TANSO-FTS measurement footprints fall."

Do the authors use glint data of TANSO-FTS?

Yes, we use the sun-glint observations over the ocean. We will make this more explicit in the text.

"and includes retrievals both over land and also over ocean when GOSAT measures in a sun-glint geometry."

Vertical profile information clarify the difference between in-situ CH4/CO2 and satellite measured column CH4/CO2. CH4/CO2 discussion using profile information from TANSO-FTS TIR band in the future might help.

Please see this section in the text:

"However, the majority of the ground-based emission ratios were derived from locations dominated by almost pure peat burning sampled close to source, whereas the space-based observations from GOSAT are derived from measurements of the smoke filling a 10.5 km diameter TANSO-FTS footprint and thus representative of much larger areas of combustion, very likely comprising a mix of peat and vegetation burning in the majority of cases."

Regarding the TIR measurements from GOSAT, we don't believe that the data quality of these products is yet at a level to be useful due to calibration issues with the spectra. In the future, or for example from GOSAT-2, being able to separate out vertical profile information through combination of the SWIR and TIR bands would prove useful for this type of work.

Atmospheric CH_4 and CO_2 enhancements and biomass burning emission ratios derived from satellite observations of the 2015 Indonesian fire plumes

Robert J. Parker[1,3], Hartmut Boesch[1,3], Martin J. Wooster[2,3], David P. Moore[1,3], Alex J. Webb[1], David Gaveau[4], and Daniel Murdiyarso[4,5]

[1]Earth Observation Science, Department of Physics and Astronomy, University of Leicester, Leicester, UK
[2]King's College London, Department of Geography, London, UK
[3]NERC National Centre for Earth Observation, UK
[4]Center for International Forestry Research, P.O. Box 0113 BOCBD, Bogor 16000, Indonesia.
[5]Department of Geophysics and Meteorology, Bogor Agricultural University, Bogor 16680, Indonesia

Correspondence to: Robert Parker (rjp23@le.ac.uk)

Abstract.

The 2015-2016 strong El Niño event has had a dramatic impact on the amount of Indonesian biomass burning, with the El Niño driven drought further desiccating the already drier than normal landscapes that are the result of decades of peatland draining, widespread deforestation, anthropogenically-driven forest degradation, and previous large fire events. It is expected that the 2015-16 Indonesian fires will have emitted globally significant quantities of greenhouse gases (GHGs) to the atmosphere, as did previous El Niño driven fires in the region. The form which the carbon released from the combustion of the vegetation and peat soils takes has a strong bearing on its atmospheric chemistry and climatological impacts. Typically, burning in tropical forests and especially in peatlands is expected to involve a much higher proportion of smouldering combustion than the more flaming-characterised fires that occur in fine-fuel dominated environments such as grasslands, consequently producing significantly more CH_4 (and CO) per unit of fuel burned. However, currently there have been no aircraft campaigns sampling Indonesian fire plumes, and very few ground-based field campaigns (none during El Niño), so our understanding of the large-scale chemical composition of these extremely significant fire plumes is surprisingly poor compared to, for example, those of southern Africa or the Amazon.

Here, for the first time, we use ~~use~~ satellite observations of CH_4 and CO_2 from the Greenhouse gases Observing SATellite (GOSAT) made in large scale plumes from the 2015 El Niño-driven Indonesian fires to probe aspects of their chemical composition. We demonstrate significant modifications in the concentration of these species in the regional atmosphere around Indonesia, due to the fire emissions.

Using CO and fire radiative power (FRP) data from the Copernicus Atmosphere Service, we identify fire-affected GOSAT soundings and show that peaks in fire activity are followed by subsequent large increases in regional greenhouse gas concentrations. CH_4 is particularly enhanced, due to the dominance of smouldering combustion in peatland fires, with CH_4 total column values typically exceeding 35 ppb above that of background "clean air" soundings. By examining the CH_4 and CO_2 excess concentrations in the fire-affected GOSAT observations, we determine the CH_4/CO_2 fire emission ratio for the entire 2-month

period of the most extreme burning (September- October 2015), and also for individual shorter periods where the fire activity temporarily peaks. We demonstrate that the overall CH_4 to CO_2 emission ratio (ER) for fires occurring in Indonesia over this time is 6.2 ppb/ppm. This is higher than that found over both the Amazon (5.1 ppb/ppm) and southern Africa (4.4 ppb/ppm), consistent with the Indonesian fires being characterised by an increased amount of smouldering combustion due to the large amount of organic soil (peat) burning involved. We find the range of our satellite-derived Indonesian ERs (6.18 ppb/ppm to 13.6 ppb/ppm) to be relatively closely matched to that of a series of "close-to-source" ground-based sampling measurements made on Kalimantan at the height of the fire event (7.53 to 19.67 ppb/ppm), although typically the satellite-derived quantities are slightly lower on average. This seems likely to be because our field sampling mostly intersected smaller-scale peat burning plumes, whereas the large-scale plumes intersected by the GOSAT TANSO-FTS footprints would very likely come from burning that was occurring in a mixture of fuels that included peat, tropical forest and already cleared areas of forest characterised by vegetation types that are more fire-prone than the natural rainforest biome (e.g. post-fire areas of ferns and scrubland, along with agricultural vegetation)

The ability to determine large-scale emission ratios from satellite data allows the combustion behaviour of very large regions of burning to be characterised and understood in a way not possible with ground-based studies, and which can be logistically difficult and very costly to consider using aircraft observations. We therefore believe the method demonstrated here provides a further important tool for characterising biomass burning emissions, and that the GHG emission ratios derived for the first time for these large-scale Indonesian fire plumes during an El Niño event, points the way to more routinely assessing spatio-temporal variations in biomass burning emission ratios using future satellite missions that will have more complete spatial sampling than GOSAT, and that will enable the contributions of these fires to the regional atmospheric chemistry and climate to be better understood.

1 Introduction

The 2015-2016 strong El Niño event, which is ongoing in the tropical Pacific at the time of writing, has had a dramatic impact on the amount of landscape burning occurring across large parts of Indonesia. Landscape fires are commonly used in this environment to clear forest and help manage land for agriculture, but an El Niño-driven drought has further dried out the already human-modified landscapes of Central Kalimantan and south Sumatra. These regions are already more flammable than their natural state due to decades of peatland draining and deforestation, anthropogenically-driven forest degradation, as well as the legacy of previous large fire events (Wooster et al., 2012). Even short localised fire events in these environments can lead to significant greenhouse gas (GHG) emissions, as demonstrated by Gaveau et al. (2014) who report that a one week fire event in Riau Province (Sumatra) was responsible for emitting 172 $\pm$ 59 Tg CO_2-eq., approximately 5-10% of Indonesia's average annual GHG emissions. The 2015 El Niño-driven fire season in Indonesia is already known to have been far more extensive than in 'normal' years (Voiland, 2016), and during the last very strong El ~~nino~~ Niño (1997-98; the strongest yet on record) massive increases in Indonesian fire activity were similarly recorded (Wooster et al., 1998; Page et al., 2002). Indeed all previous El Niño events, back to the next strongest event after 1997-98 (i.e. that of 1982-83), appear to have produced

significant increases in burning over Indonesia, as detailed in Wooster et al. (2012). Whilst the degree of fire activity increase associated with El Niño is possible to gauge using, for example, satellite-derived active fire counts, forest cover change or burned area maps (e.g. Trigg et al. (2006); Langner et al. (2007); Langner and Siegert (2009); Wooster et al. (2012)), what is equally valuable is information on the emissions to the atmosphere resulting from these burns, so that their atmospheric impacts can be more fully determined.

Using satellite-derived estimates of burned area along with assumptions on peatland 'depths of burn', Page et al. (2002) estimated that the 1997 El Niño-driven Indonesian fires released an amount of carbon (0.81-2.57 Pg) equivalent to between 13 and 40% of that year's annual global carbon emissions from fossil fuels, contributing to the largest annual increase in atmospheric CO_2 concentration detected since records began in the 1950s (Wang et al., 2013). More recently, van der Werf et al. (2010) have reported similarly anomalous estimates for that year's Indonesian burning, based on related methodologies but different datasets, and anomalies in both inter-annual variability and the atmospheric growth rates of CO_2 and CH_4 continue to be attributed to biomass burning events, including El Niño-driven Indonesian fires (Kasischke and Bruhwiler, 2002; van der Werf et al., 2004; Simmonds et al., 2005). It is possible that the 2015-16 El Niño-driven Indonesian fires, which at the time of writing have largely ceased due to heavy rains (but which may well return in 2016), may ultimately be of a similarly anomalous magnitude to those driven by prior El Niño events. There therefore exists a strong interest in both quantifying the amount of fire activity occurring and in calculating the overall carbon emissions to the atmosphere that result. Furthermore, the types of biomes being affected are important, because whilst post-fire vegetation regrowth in fire-affected areas does subsequently take up some of the released carbon, areas of burned tropical forest are often replaced by plants holding far less carbon per unit area, and the burning of peat represents an effectively permanent transfer of carbon from the land to the atmosphere (Page et al., 2002). The form in which the carbon is emitted into the atmosphere also has a strong bearing on the emission impacts, with most carbon being released as either the long-lived GHG carbon dioxide, the shorter-lived but much stronger GHG methane, or the air pollutant carbon monoxide (Andreae and Merlet, 2001). Typically, burning in tropical forests and especially in peatlands is expected to involve a much higher proportion of smouldering combustion than the more flaming-characterised combustion that occurs in fine-fuel dominated environments such as grasslands (Christian et al., 2007; Liu et al., 2014). Hence, fires in peatlands and tropical forests are expected to produce more CO and CH_4 per unit of fuel burned, with a consequent reduction in the amount of CO_2. However, currently the only information on emissions make-up in fires in Indonesian biomes come from relatively few lab-based studies where samples of fuels have been burned in combustion chambers (i.e. Christian et al. (2003); Othman and Latif (2013); Liu et al. (2014)). At present there are no known field-based studies of emissions make-up, certainly none conducted during El Niño years where the dry conditions may promote different combustion behaviour than occurs under more 'normal' meteorological and fuel moisture conditions, and none where the constituents of the large-scale plumes that most likely contain the bulk of the emitted gases (and aerosols) are assessed. The latter point is important because whilst ground-based sampling can measure emission make-up close to source, including in the field under real landscape combustion conditions, such an approach is by necessity limited to capturing smoke from individual fire locations, and usually from smaller fires, and these measurements may not fully represent the emissions characteristics of the type of large-scale plumes that may actually be responsible for holding most of the combustion products. Aircraft sampling

can provide a means to capture the latter's characteristics (e.g. Yokelson et al. (1999)), but such campaigns are costly, infrequent and logisitically challenging. An alternative approach to characterising the emission make-up of large-scale fire plumes is via satellite based sounding of wildfire plume chemistry, which has so-far been demonstrated only a few times, by Coheur et al. (2009) using IASI onboard METOP and by Ross et al. (2013) using the TANSO-FTS instrument onboard the Greenhouse gases Observing SATellite (GOSAT). Here we build on the latter work to exploit GOSAT's observations of CH_4 and CO_2 over the 2015 El Niño-driven Indonesian fires, using these to demonstrate the increase in atmospheric concentrations of CH_4 and CO_2 associated with the large scale biomass burning plumes, and deriving from these observations the CH_4 to CO_2 emission ratios for these El Niño driven Indonesian fires for the first time. We compare these Indonesian fire emissions ratios to those derived from GOSAT in alternative tropical biomes having different combustion characteristics (southern African savannah and the Amazon basin). In combination with Fire Radiative Power (FRP) and atmospheric carbon monoxide data taken from the new Copernicus Atmosphere Service Global Fire Assimilation System (CAMS-GFAS (2016)) we demonstrate the Indonesian fires are occurring in peatland dominated landscapes that explain certain characteristics of the noted emission ratios, which are themselves important in determining the so-called emissions factors representative of the combustion processes occurring in these very large-scale landscape fires.

Emissions factors (EFs) are necessary when converting estimates of the amount of fuel burned (obtained from burned area or FRP-based methods) into a quantity of each trace gas (Koppmann et al., 2005; Reid et al., 2005). These EFs are themselves often calculated through the use of emission ratios (ER) which are determined from the ratio of the excess concentrations emitted from wildfires (Andreae and Merlet, 2001). Whilst the emission factors are only one aspect of calculating the overall emitted amounts, due to the fact that satellite observations of burned area and FRP have significantly improved in recent years, the accuracy of the emission factors is becoming more crucial to the overall accuracy of the emissions (Van Leeuwen and Van Der Werf, 2011). The capability to measure the CH_4/CO_2 ERs from a variety of wildfires in different biomes across the globe, consistently using a single instrument/approach and from very large scale plumes that represent some of the largest individual fires emissions sources, is therefore a significant advancement. We first demonstrated this capability in Ross et al. (2013), and here we focus on extending this determination of satellite-derived CH_4/CO_2 ERs to Indonesia during the anomalously large El Niño-driven fire season of September-October 2015. The emissions ratios themselves are of clear interest in helping to determine the relative amounts of these two key GHGs released by the fires, but also the relative amounts of CH_4 and CO_2 being released in a smoke plume are known to vary with the dominance of smouldering and flaming combustion of the causal fire, as do the more commonly used CO_2 and CO measures (e.g. Lobert and Warnatz (1993), Yokelson et al. (1996), Wooster et al. (2011)). Furthermore, knowledge of the relative amounts of these two phases of combustion are known to exert strong controls on the relative emissions of many other compounds (e.g. Yokelson et al. (1996), Cofer et al. (1998), Lee et al. (2010)), and thus if we can better understand the relative CO_2 and CH_4 emissions makeup of the large-scale plumes emanating from these fires this may provide useful information to better estimate the type of combustion occurring and thus potentially the overall emissions characteristics beyond the two species observed.

2 El Niño and Indonesian Fire Activity

El Niño describes a large-scale climate anomaly that typically occurs once or twice per decade, with one of the key characteristics being significantly warmer than normal sea surface temperatures (SSTs) in the equatorial eastern Pacific Ocean (Trenberth, 1997). The many other effects associated with an El Niño event are complex and not always consistent between different El Niños, but most events are accompanied by warmer temperatures across much of South America, Africa, South-East Asia and Western Europe, decreased precipitation over central/southern Africa, central America, South-East Asia, and increased precipitation over the southern United States and Western Europe (Hartmann et al., 2013). Indonesia is located in the equatorial region and can be particularly affected by El Niño events, for example usually experiencing warmer temperatures and significant reductions in rainfall that exacerbate certain aspects of a landscape already heavily modified by human actions. In particular, much of the low lying land on the Indonesian islands of Sumatra and Kalimantan that was originally covered by moist, forested peatlands has been cleared and drained for agriculture, and this has led to much drier landscape conditions. Fire is commonly used to manage the land, and during the droughts associated with El Niño the already heavily disturbed peatland landscapes can become so dry that they can be ignited from the vegetation fires that are widespread even in "normal" years (Gaveau et al., 2014). Such fires can burn down into the carbon rich peat for weeks, whilst also spreading across the landscape to ignite new areas - including spreading into areas of remaining tropical forest that normally are not prone to fire. During El Niño these peat and forest fires can thus affect areas that are very much larger than those burned during "normal" years, particularly during the strongest El Niño events when fire activity can be more than an order of magnitude higher (van der Werf et al., 2008; Wooster et al., 2012). As described in Section 1, during the 1997-98 El Niño, fires in Indonesia are estimated to have released huge amounts of carbon in to the atmosphere and because of the smouldering nature of peat (and to some extent tropical forest as well), a greater proportion of these emissions are likely to be in the form of non-CO_2 gases, primarily the air pollutant CO and the strong greenhouse gas CH_4, than is the case for flaming fires (Christian et al., 2003, 2007). This contrasts with the burning of the El Niño dried finer fuels which will typically burn primarily via flaming combustion and thus release a lower proportion of CO and CH_4 and a higher proportion of CO_2 whose global warming potential is significantly lower than that of methane (Myhre et al., 2013). It is estimated that approximately 3/4 of the fire activity over this time period was due to peatland burning (Huijnen et al., 2016) .

2.1 Magnitude of El Niño Events and the Associated Fire Activity

There are many different ways to quantify the magnitude of an El Niño event but one of the most widely accepted is the Multi-Variate ENSO Index (MEI) (Wolter and Timlin, 1998). This is based on observations of a variety of meteorological parameters over the tropical Pacific Ocean. By this metric (Wolter, 2016), the current El Niño event that we are experiencing (2015/2016) is already the third strongest event on record (behind 1997/98 and 1982/83), with the potential to be classified even higher before it is complete.

To investigate the magnitude of the increased fire activity over Indonesia that has been associated with the current El Niño we examined the ~~fire radiative power (FRP)~~ Fire Radiative Power being released from the identified combustion zones. FRP is

a measure of a fires release rate of thermal radiation, and is strongly related to the rate of fuel consumption and trace gas and aerosol emission (Wooster et al., 2005; Freeborn et al., 2008). FRP is therefore both an indicator for the presence of fire, and an estimator for the amount of material being emitted to the atmosphere from that fire. Global satellite observations of FRP are made from the MODIS instruments onboard the NASA Terra and Aqua satellites at a nadir spatial resolution of 1 km, and these are incorporated into the Copernicus Atmosphere Monitoring Services (CAMS) Global Fire Assimilation System (GFAS), set up under the Monitoring Atmospheric Composition and Climate (MACC) series of research projects (CAMS-GFAS (2016)). Using FRP data converted to "FRP density" by dividing by the grid cell area (0.1°x0.1°) and adjusting for the impact of unseen parts of the land surface due to gaps in satellite coverage and variations in cloud cover (Kaiser et al., 2012), GFAS produces estimates of trace gas emissions from the mapped fire affected areas, which CAMS then uses in its atmospheric chemistry transport model to identify atmospheric abundances of the released chemical species.

Figure 1 shows the monthly total FRP density (in W/m^2) over the Indonesian region (defined as 5°N-10°S, 90°E-150°E) for the last seven years calculated from the GFAS data, including adjustments for observation frequency and cloud cover (Kaiser et al., 2012). Whilst significant landscape burning takes place every year between July and October in this Indonesian region, the fires that took place in the latter part of 2015 (particularly September and October 2015) were clearly of an extreme magnitude, with the cumulative FRP density for October 2015 exceeding 7500 W/m^2, compared to the second highest value of just over 2000 W/m^2 (October 2014).

Whilst FRP gives an indication of the intensity of fires and their associated emissions to the atmosphere, the number of fires is also a useful indicator of fire activity, especially in regions which may see many small fires as opposed to fewer, but larger, events (Wooster and Zhang, 2004; Schroeder et al., 2014). For this reason, the original MODIS MOD14/MYD14 fire counts were also examined (Giglio et al., 2003). The number of fires observed by MODIS across Indonesia during September/October 2015 are shown in Fig. 2. Overlain onto this in green are the locations of known peatlands in Sumatra, Kalimantan and Papua (Ritung et al., 2016) . It is clear that the majority of the most fire affected regions of Indonesia during the September and October 'extreme fire event', i.e. Central Kalimantan and the south-east region of Sumatra, are located in areas dominated by peatlands.

2.2 Fire Emissions and Combustion Regimes

As already stated, in contrast to the flaming combustion involved in the burning of wood/grass, peatland fires are typically dominated by deeper smouldering combustion. As smouldering combustion is less efficient than flaming combustion, there is a higher proportion of CO, CH_4 and other non-methane hydrocarbons (NHMCs) released compared to CO_2 (Bertschi et al., 2003; Yokelson et al., 2008; Wooster et al., 2011).

A literature review of previous ground and aircraft based measurements of the CH_4/CO_2 ER indicates a wide range of values, demonstrating the variability that can be dependent on not only the fuel type but also on additional factors such as fuel moisture content, the ratio of living to dead matter and how recently the area last burned (Korontzi et al., 2003). To take just one example, Koppmann et al. (1997) present CH_4/CO_2 ER values for flaming fires of 2.6 ppb/ppm from sugar cane fields, increasing to 10.3 ppb/ppm over fires dominated by smouldering combustion in forest and shrubland. Fires with intermediate

values were reported to represent a mixture of smouldering and flaming combustion. Similarly, Hurst et al. (1994) report mean ER values of 2.1 $\pm$ 1.5 ppb/ppm for flaming combustion, 5.3 $\pm$ 2.0 ppb/ppm for mixed combustion and 10.1 $\pm$ 3.9 ppb/ppm for smouldering combustion. A further study, (Bonsang et al., 1995), present values of 3.2-4.6 ppb/ppm for flaming combustion, increasing to 7.8 ppb/ppm for smouldering combustion in savannah/forest regions. The wide range of CH_4 to CO_2 emission ratios reported by these different studies demonstrates that, even when measured close-to-source as all these were, there is a high degree of variability intrinsic to the CH_4/CO_2 ER but the relative behaviour remains consistent, namely that flaming processes produce smoke with a lower CH_4 to CO_2 ratio than smouldering processes, and thus it maybe possible to distingush between these two types of combustion using measurments of this ratio.

The objectives of this work are to first determine whether the expected high concentrations of CH_4 emitted by the extreme peatland burning in September/October 2015 over Indonesia are observable from satellite data and if that is the case, to then determine the CH_4/CO_2 emission ratio of the resulting large-scale smoke plumes and compare this to measurements made in-situ. The capability to examine the large-scale emission ratios of a region such as this is important because if GOSAT can measure CH_4/CO_2 emission ratios, such observations contain information related to the mix of combustion types occurring and can thus help discriminate predominantly smouldering from predominantly flaming regions. Not only is this of direct interest for the CH_4 and CO_2 emissions themselves but is also useful when considering the many other species contained within the smoke, because the relative abundance of most of these is in part dependent on the amount of flaming and smouldering combustion occurring.

This work is presented as follows. Section 3 introduces the GOSAT satellite data used in this work, providing details on the retrieval method and how the CH_4/CO_2 data has been used to determine fire emission ratios. Section 4 describes the methodology used for determining whether a GOSAT sounding is affected by fire and provides statistics on the number of fire-affected soundings that we observe over the Indonesian fire region. Section 5 goes on to examine the enhancement in CH_4 as observed from the fire-affected data while Section 6 then uses these data to determine CH_4/CO_2 fire emission ratios, comparing them to in-situ observations of the same El Niño driven fire event. Finally we summarise our findings and comment on the outlook for further study in this area of research.

3 GOSAT Proxy XCH_4 Data

GOSAT was the first dedicated greenhouse gas measurement mission based on an Earth Observation satellite approach, and was launched by the Japanese Space Agency (JAXA) on 23rd January 2009 (Kuze et al., 2009). GOSAT is equipped with two instruments. The first is the Thermal And Near infrared Sensor for carbon Observations - Fourier Transform Spectrometer (TANSO-FTS), which provides point-based measurements of total column CO_2 and CH_4 with near-surface sensitivity because of its use of shortwave infrared (SWIR), as well as a thermal infrared (TIR) band sensitive to the mid-troposphere. The second is the Cloud and Aerosol Imager (TANSO-CAI), which provides multispectral imagery ~~that gives~~ at 0.5 km resolution with bands at 0.38 μm, 0.67 μm, 0.87 μm and 1.6 μm. This allows additional cloud/aerosol information about the region of interest within which the TANSO-FTS measurement footprints fall.

The TANSO-FTS measurement pattern originally consisted of 5 (later changed to 3) across-track points with a footprint of ~10.5 km, each separated by approximately 100 km on the ground. GOSAT also has capabilities for agile-pointing, allowing both target mode and observations of the glint spot over the ocean. Near-surface sensitivity to the target gases is achieved by the TANSO-FTS instrument utilising three SWIR spectral bands at 0.76, 1.6 and 2.0 μm, with mid-tropospheric sensitivity available from a fourth band operating between 5.5 and 14.3 μm in the TIR. Kuze et al. (2016) provide extensive details of the performance and operation of the TANSO-FTS instrument over the past 6 years. In short, although GOSAT has experienced three major anomalies over its lifetime (a solar paddle failure in May 2014, a pointing system issue in January 2015, and a cryo-cooler restart in ~~August~~ September 2015) it continues to operate well, providing high-quality atmospheric radiance measurements from which we are able to retrieve dry-air column-averaged fractions of CO_2 and CH_4 (denoted as XCO_2 and XCH_4, respectively).

Details of the University of Leicester Proxy XCH_4 GOSAT retrieval, including recent updates and uncertainty characterisation, can be found in Parker et al. (2011, 2015). In brief, the retrieval utilises the original Orbiting Carbon Observatory (OCO) "full physics" (so-called as the radiative transfer attempts to explicitly model the physical behaviour of the aerosol-scattered light) retrieval algorithm (Boesch et al., 2011; Cogan et al., 2012; O'Dell et al., 2012) developed to obtain XCO_2 from a simultaneous fit of NIR/SWIR O_2 and CO_2 bands and subsequently modified to operate on GOSAT spectral data to retrieve XCH_4 using the light-path proxy approach. Developed by Frankenberg et al. (2006) for use on SCIAMACHY data, this proxy method utilises the fact that the majority of the influence of atmospheric scattering on the retrieved XCH_4 can be negated through the co-retrieval of the spectrally close 1.6 μm CO_2 band, since the signal related to both species undergo the same light-path enhancement through scattering. The resulting XCH_4/XCO_2 ratio is therefore robust to the effects of aerosol. Generally the final Proxy XCH_4 is obtained via the application of XCO_2 model fields to this ratio. Typically due to the fact that there is significantly less influence from aerosol on the final product than with the typical "full physics" retrieval approach (Butz et al., 2010), high-quality retrievals are possible even under cloud/aerosol conditions where the typical full physics retrieval struggles. Not only does this result in many more successful soundings globally, it also allows studies over cloudy or smoke-affected regions where no data at all may be available from the typical "full physics" retrieval approach.

XCH_4 data obtained using the Proxy approach described above have been used in many inversion studies (Fraser et al., 2013; Wecht et al., 2014; Fraser et al., 2014; Cressot et al., 2014; Alexe et al., 2015; Turner et al., 2015) to estimate both global and regional emissions of XCH_4. Normally the main disadvantage of the Proxy XCH_4 retrieval is that it requires an accurate and unbiased XCO_2 model to convert the ratio back into XCH_4 (Schepers et al., 2012). However, in our current study of the atmospheric impacts and emission ratios of the El Niño driven fires in Indonesia, we use only the individual retrieved XCH_4 and XCO_2 components of the Proxy retrieval and hence, have no dependence on any CO_2 model. For the purposes of this study, the standard GOSAT Proxy data record (typically generated as part of the ESA GHG-CCI project (Buchwitz et al., 2015), 4-6 months behind real time due to the use of ECMWF ERA-Interim data in the processing chain) has been extended with the use of ECMWF Analysis data in order to produce results more quickly than are possible with the normal route. In this way, the Proxy XCH_4 timeseries has been extended from June 2015 to November ~~2015.~~ 2015 and includes retrievals both over land and also over ocean when GOSAT measures in a sun-glint geometry.

In Section 1, it was shown that September/October 2015 exhibited significantly higher FRP over Indonesia than previous years. Before exploring the GOSAT data over Indonesia in more detail, it is first useful to put the GHG observations for September and October 2015 into the context of the longer GOSAT timeseries. Figure 3 shows the 95th-percentile values for the monthly GOSAT data over Indonesia for the entire data record from April 2009 to November 2015. The upper panel shows the XCH_4/XCO_2 ratio, with the central and lower panels showing the individual XCH_4 and XCO_2 respectively.

In order to quantify the extreme nature of the October 2015 observations and to account for the annual growth rate, we define the magnitude of the enhancement as the October-July difference for each year, with July typically signifying the start of the fire season in this region. For CO_2 we observe a magnitude of 4.35 ppm for October 2015 compared to a mean value of 1.05 $\pm$ 1.42 ppm for the previous years (2009-2014). In the case of XCH_4, the enhancement value for October 2015 is found to be 45.65 ppb compared to an average for previous years of 11.93 $\pm$ 3.60 ppb. The enhancement of both the XCO_2 and, in particular, XCH_4 in October 2015 is therefore significantly higher than that observed over the region in previous years, corresponding to the extreme in fire activity observed in Fig. 1.

4 Identifying Fire-Affected GOSAT Soundings

Section 3 established that a significant increase is observed in the monthly maximum values for the XCH_4, XCO_2 and the XCH_4/XCO_2 during September/October 2015 (calculated as the 95th-percentile values) recorded over Indonesia by GOSAT. To further investigate the atmospheric GHG anomalies identified over Indonesia by GOSAT in Figure 3, it is first necessary to identify which GOSAT soundings are directly affected by fire emissions, and which can be considered "background" (clear) cases

We use the CAMS CO fields to determine if a particular GOSAT sounding is likely to be fire affected. In addition to emissions from CO sources and their atmospheric transport, the CAMS CO fields incorporate carbon monoxide total column measurements from the IASI and MOPITT instruments (Inness et al., 2015). We sampled the CO fields at the time/location of each GOSAT sounding, and based on the CO distribution and data from the GOSAT Cloud and Aerosol Imager~~(CAI)~~, values in excess of 0.003 kg/m^2 were determined as being likely affected by the local fire emissions. Conversely, if the CO value was less than 0.00075 kg/m^2 then the sounding was classed as "clear" (i.e. unaffected by local fire emissions). GOSAT soundings corresponding to locations and times having CO values between these thresholds were not able to be confidently classed as either "fire affected" or "clear". Out of 3946 GOSAT soundings over Indonesia during September/October 2015, the CAMS CO identifies 341 (8.6%) of these as being affected by fire and 1272 (32.3%) as clear (i.e. unaffected by fire), and with the remainder lying between these thresholds.

Figure 4 shows a GOSAT CAI false-colour image covering much of Kalimantan on 21st October 2015, a time when a massive pall of smoke enveloped Central Kalimantan and parts of the surrounding regions. The active fire detections for this day made from MODIS are also shown (small purple circles), along with the numbered locations of the individual GOSAT TANSO-FTS soundings (red circles). All GOSAT soundings made co-incident with this CAI image were in locations where the simultaneous CAMS CO field indicated the corresponding TANSO-FTS measurement was 'fire affected'.

5 Observations of Enhanced Methane Concentrations

Once we had identified a set of GOSAT soundings that were able to be clearly classed as "fire affected" or "clear", it became possible to examine the XCH_4, XCO_2 and XCH_4/XCO_2 distributions in order to determine the changes in the column amount and trace gas ratio characteristics related to the extreme levels of fire activity. Figure 5 shows histograms of the XCH_4/XCO_2 ratio, as well as the individual XCH_4 and XCO_2 components, for all the "clear" (blue) and "fire affected" (red) soundings, as well as for the entire dataset (green).

As Table 1 shows, for the XCH_4/XCO_2 ratio, the mean ratio calculated from all the data is 4.54 ppb/ppm, with a standard deviation of 0.033 ppb/ppm. The histograms for the clear and fire-affected data show two clearly separated distributions, with means of 4.52 and 4.59 ppb/ppm respectively. When examining just the XCO_2 distributions, there appears to be less of a distinct separation, with means of 399.9 and 401.1 ppm respectively for the clear and fire-affected cases. This corresponds to a XCO_2 increase of 0.3% percent over the background XCO_2 concentrations, whereas the XCH_4 distribution for the fire-affected scenes shows a much larger mean enhancement of 1.9% percent over the background (1840.1 ppb vs 1805.5 ppb).

In order to examine the spatial distribution of the atmospheric GHGs and XCH_4/XCO_2 ratio enhancements, Figure 6 shows (top to bottom) maps of the GOSAT-retrieved XCH_4, XCO_2, XCH_4/XCO_2 ratio, along with the CAMS total column CO and IASI total column CO for all TANSO-FTS sounding locations (left), "clear" locations (centre) and "fire-affected" locations (right). These data show that the spatial extent of the enhancements in XCH_4, XCO_2 and in the resulting XCH_4/XCO_2 ratio, as well as in the CAMS and IASI CO, are related to the enhanced fire activity seen over parts of Sumatra and Kalimantan (shown in Fig. 2), whose emissions are being transported primarily westwards over the ocean (last column of Fig. 6).

This finding confirms that the anomalously large amount of fire activity seen occurring in September and October 2015 during the El Niño (Fig. 1) and which included fires in the extensive peatlands of Central Kalimantan and south Sumatra (Fig. 2) resulted in a significant increase in atmospheric column amounts of CH_4 and CO_2 downwind of the fires. These enhancements are observable from GOSAT satellite observations, and in the following section we examine the CH_4/CO_2 emission ratio (ER) of this smoke to better understand the combustion characteristics.

6 Determination of CH_4/CO_2 Emission Ratios

As discussed in Section 2, the capability to determine large-scale regional emission ratios during intense fire-activity is important as it allows information to be gained not only on the emissions of these gases themselves but also potentially on the relative dominance of flaming vs. smouldering combustion. Our previous work Ross et al. (2013) demonstrated for the first time an ability to determine CH_4/CO_2 fire emission ratios from satellite data, in that case using GOSAT to study ERs of boreal forest (Canada/Russia), tropical forest (Brazil) and savannah (Southern Africa) fires. The satellite-derived emission ratios obtained appeared to be in good agreement with those derived during ground and aircraft sampling studies in the same biomes, albeit these in-situ data themselves show relatively large variations. Such variability is likely a function of differences in fuel type, fuel moisture and fire behaviour that occurred between different measurement campaigns, fire locations and time of year or day (Van Leeuwen and Van Der Werf, 2011). Here we apply the technique of Ross et al. (2013) to our current GOSAT Proxy

retrievals of XCO_2 and XCH_4 made during the September-October 2015 Indonesian fires, in order to determine the emission ratios characterising the very large scale plumes seen during this anomalously large climate-related fire event.

As a first step in this process, it is useful to calculate the excess (or "Δ") XCH_4 and XCO_2 values prior to any subsequent processing, since for example the fire emissions can be superimposed into a "background" atmosphere that itself contains spatially and/or temporally varying amounts of XCH_4 and XCO_2. Calculating such excess amounts removes the impact of potentially varying background concentrations. However, since we utilise the XCH_4 and XCO_2 components of the GOSAT Proxy XCH_4 retrieval, which themselves do ~~no~~ not account explicitly for aerosol scattering (but instead relying on these effects to ratio out when computing the final Proxy XCH_4 values; see Section 3) this does provide some potential for error to be introduced in any subsequently calculated CH_4/CO_2 emissions ratio. Such errors are related to the fact that the degree of scattering may be different between the "fire affected" (i.e. smoke laden) and matching background (i.e "clear") TANSO-FTS soundings from which the excess amounts are calculated. We analysed the magnitude of this effect using a simple model, included as Appendix A, and the results indicate that it is possible to underestimate the CH_4/CO_2 emission ratio by around $\sim$10% if appropriate care is not taken during selection of the 'clear' soundings whose column amounts are to be subtracted from those of the "fire affected" soundings in order to calculate the excess column amounts. In a region such as Indonesia during El Niño, where large-scale fire activity is clearly greatly affecting the aerosol composition of the local atmosphere, this aspect becomes even more challenging. To deal with this, we only used fire affected TANSO-FTS soundings made over land, so as to minimise the effect of mixing/dilution as smoke-laden air was transported longer distances over the ocean. For each fire-affected sounding a matching background measurement was selected from the group of "clear" soundings located over the same island and as close as possible to the fire-affected measurement (e.g. the background for the Sumatra soundings were selected from clear soundings between 90°E-108°E and 5°N-10°S) in order to minimise impacts stemming from use of non-uniform background measurements as detailed in Yokelson et al. (2013). Out of 131 fire-affected soundings, a suitable background sounding was identified for 105 (80%) of the soundings. Each background XCH_4 and XCO_2 value was then subtracted from the concentration derived from its corresponding fire-affected sounding in order to produce the ΔXCH_4 and ΔXCO_2 values, from which the emission ratios could then be calculated.

Figure 7 shows the ΔXCH_4 values plotted against the simultaneously derived ΔXCO_2 values for all of the fire-affected soundings measured over Indonesia for the September-October 2015 period. The CH_4/CO_2 emission ratio derived from the linear best fit to these data is 6.2 ppb/ppm (correlation coefficient of 0.937). Whilst this calculated CH_4/CO_2 emission ratio is significantly above that of the ambient background ($\sim$4.52 ppb/ppm), the many fire plumes sampled by GOSAT soundings across the September-October 2015 period mean that potential variations in the emissions ratios over time (and space) can also be explored. Figure 8 once again shows the daily CAMS FRP density data, but this time for September-October 2015 only and as a daily average for the entire Indonesian region as well as for Sumatra and Kalimantan individually. There is very significant variability seen in the fire activity across these two months, and we identify several distinct time periods to examine in more detail for both Sumatra and Kalimantan. The period 9th - 15th September over Sumatra is characterised by a steady increase in FRP density, peaking on 12th September at over 200 W/m^2 before decreasing again and reducing to below 50 W/m^2 by 15th September and we take this as Period 1 for Sumatra. By contrast, over Kalimantan at around the

same time (specifically between the 8th and 17th September) there is a peak in FRP on 8th September of nearly 300 W/m^2, followed by a lull around the middle period before a second increase to almost 150 W/m^2 on 13th/14th September. We take this as Period 1 for Kalimantan. In contrast to the differing behaviours during Period 1, both Sumatra and Kalimantan exhibit somewhat more similar trends in fire activity during Period 2, starting with a high peak (over 300 W/m^2) on 19th and 14th October for Sumatra and Kalimantan respectively, however while over Kalimantan the fire activity then immediately reduces to a lower level (around 100 W/m^2), over Sumatra high FRP density values in excess of 300 W/m^2 are maintained over several days before slowly decreasing. This suggests a significantly larger fire event over Sumatra than over Kalimantan at this time, a finding consistent with the CAMS total column CO fields (e.g. as seen in Fig. 6). Although Fig. 8 suggests that an additional period centred around 22nd September should be of interest, there are insufficient GOSAT soundings during this time from which to determine an ER, demonstrating that the somewhat limited GOSAT sampling strategy can lead to a sparseness of observations in certain situations.

Figure 9 shows the ΔXCH_4 vs ΔXCO_2 measurements recorded over Sumatra, for the entire 2-month period (Sept - Oct) (top), and for Period 1 (middle) and Period 2 (bottom) only. Over the two months, a total of 66 fire-affected TANSO-FTS measurements are identified that have a suitable matching background available from which to calculate ΔXCH_4 and ΔXCO_2. The linear best fit to these data give a CH_4/CO_2 emission ratio of 6.64 ppb/ppm (R = 0.893) for these Sumatran fires. When examining the Periods 1 and 2 only, which Fig. 8 shows corresponds to times of increased fire activity over the Island, higher emission ratios of 8.1 and 8.8 ppb/ppm are derived (R = 0.91 and 0.92 respectively). These higher CH_4/CO_2 emission ratios are consistent with the region being characterised by a larger proportion of smouldering combustion, most likely of peatland given the preponderance of that landcover in the fire-affected area (Fig. 2), resulting in enhanced CH_4 concentrations as already observed in Section 5.

Similar to Figure 9, Figure 10 shows the ΔXCH_4 and ΔXCO_2 retrievals for Kalimantan, plotted on a scatterplot from which the CH_4/CO_2 emission ratio can be derived. Over the two months of September and October 2015, Fig. 8 shows that Kalimantan appears characterised by typically lower amounts of fire activity than Sumatra, interspersed with relatively short but intense episodes such as those on 8th September and 14th October. The CH_4/CO_2 emission ratio calculated for the Kalimantan data across the entire two month period is found to be 6.2 ppb/ppm, calculated from 39 separate ΔXCH_4 and ΔXCO_2 observations (correlation coefficient of 0.974). However, when examining Period 1 only (8th-17th September), although derived from only 9 data points (R=0.92) an extremely high emission ratio is found (13.6 ppb/ppm, R = 0.92). By contrast, during Period 2 (14th-25th October) the ER is found once again to be lower, at 6.2 ppb/ppm (R = 0.97). This lower value may be affected by the fact that throughout Period 2 extensive smoke aerosol covers much of Kalimantan (as seen in Fig. 4) and the selection of 'clear' TANSO-FTS that appropriately represent the clean background of the fire-affected measurements is significantly more difficult. This is further compounded by the fact that the wind vectors (not shown) for this period indicate that the background air is likely to be coming from further south, potentially having a different CH_4 and CO_2 concentration.

6.1 Ground Based Emission Ratios from El Niño Enhanced Peat and Vegetation Fires

In addition to space-based observations described above, during October 2015 at the height of the fire activity on Kalimantan (Fig. 8) a short field campaign was conducted to derive CH_4 to CO_2 emission ratios for comparison to the GOSAT-derived values. During this campaign, smoke was sampled and emission ratios derived for individual fire plumes stemming from the El Niño enhanced landscape fires. Trace gas mixing ratio measures of CO_2 and CH_4 were made at 1 Hz frequency in plumes from fires at four different locations within ∼30 km of Palankarya (2.21° S, 113.92° E), the capital of Central Kalimantan and one of the most fire affected regions during the 2015 El Niño related drought (Drake, 2015). We use a ground-based, more portable version of the cavity enhanced laser absorption spectrometer described in O'Shea et al. (2013). The precision (Allan variance, 1 sigma @ 1 hz) of the mixing ratios derived via the laser spectroscopy was 1.71 ppb for CH_4, and 2.63 ppm for CO_2, with a total absolute uncertainty of around 1% of the measured concentrations. Fires at the four different locations were sampled between 12th and 16th October 2015, with each site located on peat but with plumes encompassing both "pure" peat burning and also times when both peat and some overlying vegetation was being consumed. The CH_4/CO_2 emission ratios determined from these close-to-source measurements varied between 7.53 and 19.7 ppb/ppm (mean ± sd = 12.9 ± 3.9 ppb/ppm), a range relatively consistent with that determined from the GOSAT-derived space-based observations (6.18 to 13.6 ppb/ppm). However, the majority of the ground-based emission ratios were derived from locations dominated by almost pure peat burning sampled close to source, whereas the space-based observations from GOSAT are derived from measurements of the smoke filling a 10.5 km diameter TANSO-FTS footprint and thus representative of much larger areas of combustion, very likely comprising a mix of peat and vegetation burning in the majority of cases.

Despite this potential for the GOSAT-derived CH_4 to CO_2 ER to be somewhat less characteristic of "pure" peat burning than are some of the "close to source" measurements, and the potential for the measurements to be influenced by cleaner air (such as that transported from the south), it is still expected that the emissions over Indonesia will be largely dominated by smouldering combustion, resulting in a typically higher CH_4/CO_2 ER than that observed from flaming combustion as is generally characteristic of most African Savannah burning (Wooster et al., 2011). To confirm that this is the case, the same ~~GOAST-based~~ GOSAT-based analysis performed here for the 2015 Indonesian fires was also performed for southern Africa (defined as 0°N-40°S, 30°W-60°E) and the Amazon (defined as 0°N-40°S, 30°W-75°W), both of which underwent significant fire activity during this same time period. The calculated CH_4/CO_2 emission ratio for southern Africa was found to be 4.35 ppb/ppm (see Appendix B, Fig. 12), consistent with observations of flaming-dominated combustion in Savannah regions. Wooster et al. (2011), using a ground-based open path FTIR system, reported CH_4 to CO_2 ERs for different phases of southern African savannah burns conducted on 7 ha plots in Kruger National Park, South Africa. Backfires (spreading against the wind) typically produced emissions with very complete combustion characteristics, with CH_4 to CO_2 ERs of 1.9 - 2.2 ppb/ppm, apart from in one case where a value of 6.0 ppp/ppm was recorded. Residual areas of smouldering combustion present after the fire front had passed were recorded as having CH_4 to CO_2 ERs of 3.1 - 14.1 ppb/ppm, although it was possible that the lowest ERs reported were significantly influenced by remaining pockets of flaming activity. The headfire emissions which combine the smoke from the most intense flaming part of the burn with those from the "smouldering zone" immediately behind were

found to have CH_4 to CO_2 ERs of 2.4 - 5.4 ppb/ppm. The overall "fire averaged" CH_4 to CO_2 emission ratio, calculated from the ERs of the individual phases and using airborne measures of FRP to estimate the amount the fuel consumption in each for the purposes of the weighting calculation, was 4.3 $\pm$ 1.7 ppb/ppm, very close to the 4.35 ppb/ppm derived from GOSAT's observations of large-scale southern African savannah plumes. This provides further evidence for the representivity of our GOSAT approach, which is currently the only method able to assess the ERs of the largest plumes emanating from landscape fires, albeit only at the relatively sparse sampling locations targeted by GOSAT. The CH_4/CO_2 emission ratio for the Amazon is, as perhaps expected, somewhat in-between that of African savannah and Indonesian peatlands/forests, being 5.1 ppb/ppm (see Fig. 13). Guild et al. (2004) and references therein report the presence of significant smouldering combustion in Amazon fires occurring in forested regions, much more than typically seen in African savannah and primarily stemming from the coarse woody fuels that represent a significant component of the fuel in this biome. However, smouldering in the peat-dominated fuels of the Indonesian fires would still be expected to be more prevalent (Stockwell et al., 2014), and so the CH_4 to CO_2 ER would be expected to be higher there, as we have indeed found.

7 Summary and Outlook

The objective of this study was to utilise XCH_4 and XCO_2 observations made by the GOSAT satellite when passing over Indonesia to probe the composition of large-scale plumes from the 2015 Indonesian fires for the first time, these extreme fires being driven by the ongoing strong El Niño that is the largest seen since 1997-98. We wished to both identify the atmospheric greenhouse gas impacts of the very significant increase in fire activity and use any such measurements to determine the biomass burning emission ratios of these two important GHGs using the technique we pioneered in Ross et al. (2013). This would enable the characterisation of certain aspects of the chemical make-up of these large-scale El Niño driven fires for the first time, which in 1997-98 were responsible for the largest release of fire emitted GHGs seen worldwide, and indeed which are believed to be of a magnitude not seen since that period anywhere on Earth (van der Werf et al., 2010).

Our analysis of GOSAT data confirms a significant enhancement of both XCH_4 and XCO_2 in the fire-affected GOSAT soundings, with the greatest change seen in the XCH_4 mixing ratios where we see an average value of 1840.1 ppb compared to an average value in the 'clear' (non-fire affected) cases of 1805.5 ppb. For these fire-affected soundings, the CH_4/CO_2 emission ratio was estimated from the gradient of the linear best fit to the excess XCH_4 and XCO_2 values. We find an overall ER for the entire Indonesian fire-affected region during the September-October 2015 fire peak of 6.2 ppb/ppm, with Sumatra showing slightly higher mean ERs (6.6 ppb/ppm) than Kalimantan (6.2 ppb/ppm). When examining shorter periods of time to focus on specific fire episodes on each island, we find ERs as low as 6.1 and as high as 13.6 ppb/ppm. This range is consistent with that seen in field-sampled GHG data taken in October 2015 on Kalimantan, close to the fire sources, but we believe the large-scale sampling provided by the GOSAT TANSO-FTS 10.5 km diameter footprints enables sampling of a much more representative amount of smoke than does the relatively limited, small-scale sampling possible on the ground. We therefore believe that our GOSAT-derived emission ratios are well suited for use in studies attempting to understand the impact of these extreme El Niño driven fires on the larger-scale, regional atmosphere.

Our GOSAT-derived emission ratios for Indonesia indicate plumes that appear more dominated by the products of smouldering combustion than the plumes sampled by GOSAT in southern Africa and in the Amazon during the same period, consistent with prior expectation and previous ground-based and airborne sampling campaigns that suggest less smouldering dominated combustion in these latter biomes (especially in the savannah case). GOSAT's capability to determine not only the enhancement in greenhouse gas abundance stemming from such large fire events, but also to provide the data necessary to calculate the GHG emissions ratios and help identify the relative balance of smouldering and flaming activity ongoing in very large regions is an extremely valuable aid to understanding the composition of the plumes and their impact on regional atmospheric composition and climate. Some challenges remain, mainly relating to obtaining an accurate representation of the background "non-fire affected" $\mathrm{XCH_4}$ and $\mathrm{XCO_2}$ amounts (See Appendix A). However, the technique that we present here and in Ross et al. (2013) should be easily applicable to future satellite missions focused on atmospheric composition, and certain of these will have increased spatial and temporal resolutions that will greatly aid in obtaining the most suitable background observations. One such mission, Sentinel-5 Precursor, is planned for launch in 2016 and is capable of measuring both $\mathrm{CH_4}$ and CO at a high spatial resolution, providing an ability that GOSAT currently lacks. We believe therefore that this work will prove valuable in eventually facilitating the routine determination of regional biomass burning ERs from space, and their spatio-temporal variations whose importance is described in e.g. Van Leeuwen and Van Der Werf (2011). Such a capability might ultimately allow the characterisation of such burning events under different climatic and biome conditions.

Appendix A

As discussed in Section 6, there exists the potential to introduce errors into the GOSAT-derived emission ratios if the fire-affected sounding and the background sounding each contain sufficiently different aerosol scattering characteristics. As the fire-affected sounding will by definition usually contain a non-trivial amount of smoke aerosols, whilst the background sounding is in theory supposed to be smoke-free, some quantification of this affect is needed. In this section we derive and use a simple mathematical representation to determine the magnitude of such effects.

Let the observed excess concentration be the difference between the observed fire and background concentrations:

$$\Delta\mathrm{XCH_4} = \mathrm{XCH_4^{fire}} - \mathrm{XCH_4^{bgd}} \tag{A1}$$

Both soundings will have an error due to scattering associated with them which typically lengthens the light-path and hence reduces the inferred gas mixing ratio. This error factor, here termed A, will be different for the fire and background cases.

Therefore:

$$\Delta\mathrm{XCH_4} = A_{fire}\mathrm{XCH_4^{fire}} - A_{bgd}\mathrm{XCH_4^{bgd}} \tag{A2}$$

Similarly for $\mathrm{XCO_2}$ we have:

$$\Delta\mathrm{XCO_2} = A_{fire}\mathrm{XCO_2^{fire}} - A_{bgd}\mathrm{XCO_2^{bgd}} \tag{A3}$$

The ratio of the excess concentrations due to the fire emissions, from which we calculate the CH_4 to CO_2 emission ratio, is then given by:

$$\frac{\Delta \mathrm{XCH_4}}{\Delta \mathrm{XCO_2}} = \frac{A_{fire}\mathrm{XCH_4^{fire}} - A_{bgd}\mathrm{XCH_4^{bgd}}}{A_{fire}\mathrm{XCO_2^{fire}} - A_{bgd}\mathrm{XCO_2^{bgd}}} \tag{A4}$$

Now we set the observed CH4 concentration in the fire sounding to the background concentration plus the true excess concentration related to the fire:

$$\mathrm{XCH_4^{fire}} = \mathrm{XCH_4^{bgd}} + \Delta\mathrm{XCH_4^{true}} \tag{A5}$$

Doing the same for XCO_2 now gives:

$$\frac{\Delta \mathrm{XCH_4}}{\Delta \mathrm{XCO_2}} = \frac{A_{fire}(\mathrm{XCH_4^{bgd}} + \Delta\mathrm{XCH_4^{true}}) - A_{bgd}\mathrm{XCH_4^{bgd}}}{A_{fire}(\mathrm{XCO_2^{bgd}} + \Delta\mathrm{XCO_2^{true}}) - A_{bgd}\mathrm{XCO_2^{bgd}}} \tag{A6}$$

This can then be expanded to:

$$\frac{\Delta \mathrm{XCH_4}}{\Delta \mathrm{XCO_2}} = \frac{A_{fire}\mathrm{XCH_4^{bgd}} + A_{fire}\Delta\mathrm{XCH_4^{true}} - A_{bgd}\mathrm{XCH_4^{bgd}}}{A_{fire}\mathrm{XCO_2^{bgd}} + A_{fire}\Delta\mathrm{XCO_2^{true}} - A_{bgd}\mathrm{XCO_2^{bgd}}} \tag{A7}$$

and then rearranged to:

$$\frac{\Delta \mathrm{XCH_4}}{\Delta \mathrm{XCO_2}} = \frac{(A_{fire} - A_{bgd})\mathrm{XCH_4^{bgd}} + A_{fire}\Delta\mathrm{XCH_4^{true}}}{(A_{fire} - A_{bgd})\mathrm{XCO_2^{bgd}} + A_{fire}\Delta\mathrm{XCO_2^{true}}} \tag{A8}$$

Now let the ratio of the two error terms be

$$A_{ratio} = A_{fire}/A_{bgd} \tag{A9}$$

which then rearranged gives:

$$A_{fire} = A_{ratio}A_{bgd} \tag{A10}$$

Therefore

$$A_{fire} - A_{bgd} = A_{ratio}A_{bgd} - A_{bgd} = A_{bgd}(A_{ratio} - 1) \tag{A11}$$

Substituting this in now gives:

$$\frac{\Delta \mathrm{XCH_4}}{\Delta \mathrm{XCO_2}} = \frac{(A_{bgd}(A_{ratio} - 1))\mathrm{XCH_4^{bgd}} + A_{ratio}A_{bgd}\Delta\mathrm{XCH_4^{true}}}{(A_{bgd}(A_{ratio} - 1))\mathrm{XCO_2^{bgd}} + A_{ratio}A_{bgd}\Delta\mathrm{XCO_2^{true}}} \tag{A12}$$

The A_{bgd} terms cancel, giving:

$$\frac{\Delta \mathrm{XCH_4}}{\Delta \mathrm{XCO_2}} = \frac{(A_{ratio} - 1)\mathrm{XCH_4^{bgd}} + A_{ratio}\Delta\mathrm{XCH_4^{true}}}{(A_{ratio} - 1)\mathrm{XCO_2^{bgd}} + A_{ratio}\Delta\mathrm{XCO_2^{true}}} \tag{A13}$$

This equation therefore relates the observed excess concentrations (ΔXCH_4 and ΔXCO_2) calculated from the difference in GOSAT's "fire-affected" and "background" soundings to the true background concentrations (XCH_4^{bgd} and XCO_2^{bgd}), the true excess concentrations (ΔXCH_4^{true} and ΔXCO_2^{true}) and the ratio between the error terms, A_{ratio}. Furthermore, we can use this simple relationship to explore the likely error in the calculated emission ratio for a given value of A_{ratio}.

Figure 11 shows the implementation of Equation A13 for various scenarios. The background XCH_4 and XCO_2 concentrations are fixed at 1850 ppb and 400 ppm respectively, representing the normal "fire-free" atmosphere. The true methane enhancement (ΔXCH_4^{true}) is varied between 0-50 ppb in 5 ppb increments and the true emission ratio between CH_4 and CO_2 is varied between 0.003 and 0.012. The different panels then show the behaviour for various ranges of A_{ratio}. The top-left panel has A_{ratio} set at a constant value of 1 (i.e. the error in the background is exactly the same as the error in the fire cases), which is the ideal situation, and the true emission ratios are reproduced exactly. The top-right panel allows A_{ratio} to vary between 0.999 and 1.0. The effect of this is a slight "spreading" of the lines and the difference between the true and observed emission ratio is minimal. The bottom-left panel increased the range of A_{ratio} to 0.995 to 1.0 which causes the observed emission ratios to differ more from the truth, with a true emission ratio of 0.008 only appearing as an observed ratio of 0.00755, an error of 5.6%. Finally, in the bottom-right panel, the value of A_{ratio} is allowed to vary between 0.99 and 1.0. This relatively large variation decreases the observed emission ratio further, with a true emission ratio of 0.008 appearing as an observed ratio of 0.00686 for example.

Whilst there are many unknowns that impact the value of A_{ratio}, and so it is not possible to know its exact value for a particular pair of GOSAT "fire affected" and "background" observations used to derive an emissions ratio, it is possible to determine its expected range. By comparing the scatter of the fire affected and background XCH_4 values to the Proxy XCH_4 data (which is much less affected by aerosol and in this case is used as the "truth") it is possible to estimate the likely range of values of A_{ratio}. The standard deviation of the ratio between the XCH_4/Proxy XCH_4 for the background and fire cases is found to be 0.00494, suggesting that values of A_{ratio} are likely in the 0.995 to 1.0 range (i.e. up to a 0.5% reduction in A). This means that whilst we are likely to tend to underestimate the true CH_4 to CO_2 emissions ratios with GOSAT, for the majority of cases (CH_4 to CO_2 ERs in the range 0.005-0.008) the effect can be considered small, with typical biases of 0.4-5.6%. Even in extreme cases with high ERS (e.g. 0.012), we expect an error of less than 15%.

Appendix B

This section contains ΔXCH_4 vs ΔXCO_2 correlation plots for southern Africa (Fig. 12) and the Amazon (Fig. 13) as discussed in the main text in Section 6.

Acknowledgements. R. J. Parker is funded via an ESA Living Planet Fellowship with additional funding from the UK National Centre for Earth Observation (NCEO) and the ESA Greenhouse Gas Climate Change Initiative (GHG-CCI). H. Boesch, D. Moore and M. Wooster are also supported by NERC NCEO. A, J. Webb is funded by a NERC PhD. Field measurements in Indonesia were part supported by NERC grant NE/J010502/1 [NERC SAMBBA]. Field measurements were also part supported by a DFID grant to CIFOR (Project No. 203034).

Bruce Main at King's College London and Agus Salim at CIFOR are thanked for their technical contributions to the field measurement campaign. D. Murdiyarso acknowledges the support provided by USAID and USFS. This work also relates to NERC Grant NE/N01555X/1.

We thank the Japanese Aerospace Exploration Agency, National Institute for Environmental Studies, and the Ministry of Environment for the GOSAT data and their continuous support as part of the Joint Research Agreement. We also thank CAMS for provision of the data from GFAS. We also acknowledge the use of MODIS Active Fire Detections extracted from MCD14ML distributed by NASA FIRMS (available on-line [https://earthdata.nasa.gov/active-fire-data]). We thank EUMETSAT for the IASI CO Level 2 data. IASI is a joint mission of EUMETSAT and the Centre National d'Études Spatiales (CNES, France).

Finally, this research used the ALICE High Performance Computing Facility at the University of Leicester.

References

Alexe, M., Bergamaschi, P., Segers, A., Detmers, R., Butz, A., Hasekamp, O., Guerlet, S., Parker, R., Boesch, H., Frankenberg, C., Scheepmaker, R., Dlugokencky, E., Sweeney, C., Wofsy, S., and Kort, E.: Inverse modelling of CH4 emissions for 2010-2011 using different satellite retrieval products from GOSAT and SCIAMACHY, Atmospheric Chemistry and Physics, 15, 113–133, doi:10.5194/acpd-14-11493-2014, 2015.

Andreae, M. O. and Merlet, P.: Emission of trace gases and aerosols from biomass burning, Global biogeochemical cycles, 15, 955–966, doi:10.1029/2000GB001382, 2001.

Bertschi, I. T., Yokelson, R. J., Ward, D. E., Christian, T. J., and Hao, W. M.: Trace gas emissions from the production and use of domestic biofuels in Zambia measured by open-path Fourier transform infrared spectroscopy, Journal of Geophysical Research: Atmospheres, 108, doi:10.1029/2002JD002158, 2003.

Boesch, H., Baker, D., Connor, B., Crisp, D., and Miller, C.: Global Characterization of CO2 Column Retrievals from Shortwave-Infrared Satellite Observations of the Orbiting Carbon Observatory-2 Mission, Remote Sensing, 3, 270–304, doi:10.3390/rs3020270, 2011.

Bonsang, B., Boissard, C., Le Cloarec, M., Rudolph, J., and Lacaux, J.: Methane, carbon monoxide and light non-methane hydrocarbon emissions from African savanna burnings during the FOS/DECAFE experiment, Journal of atmospheric chemistry, 22, 149–162, doi:10.1007/BF00708186, 1995.

Buchwitz, M., Reuter, M., Schneising, O., Boesch, H., Guerlet, S., Dils, B., Aben, I., Armante, R., Bergamaschi, P., Blumenstock, T., Bovensmann, H., Brunner, D., Buchmann, B., Burrows, J., Butz, A., Chadin, A., Chevallier, F., Crevoisier, C., Deutscher, N., Frankenberg, C., Hase, F., Hasekamp, O., Heymann, J., Kaminski, T., Laeng, A., Lichtenberg, G., Maziere, M. D., Noel, S., Notholt, J., Orphal, J., Popp, C., Parker, R., Scholze, M., Sussmann, R., Stiller, G., Warneke, T., Zehner, C., Bril, A., Crisp, D., Griffith, D., Kuze, A., O'Dell, C., Oshchepkov, S., Sherlock, V., Suto, H., Wennberg, P., Wunch, D., Yokota, T., and Yoshida, Y.: The Greenhouse Gas Climate Change Initiative (GHG-CCI): Comparison and quality assessment of near-surface-sensitive satellite-derived {CO2} and {CH4} global data sets, Remote Sensing of Environment, 162, 344 – 362, doi:http://dx.doi.org/10.1016/j.rse.2013.04.024, 2015.

Butz, A., Hasekamp, O. P., Frankenberg, C., Vidot, J., and Aben, I.: CH4 retrievals from space-based solar backscatter measurements: Performance evaluation against simulated aerosol and cirrus loaded scenes, Journal of Geophysical Research D: Atmospheres, 115, doi:10.1029/2010JD014514, 2010.

CAMS-GFAS, E.: CAMS Global Fire Assimilation System, http://apps.ecmwf.int/datasets/data/cams-gfas/, 2016.

Christian, T. J., Kleiss, B., Yokelson, R. J., Holzinger, R., Crutzen, P. J., Hao, W. M., Saharjo, B. H., and Ward, D. E.: Comprehensive laboratory measurements of biomass-burning emissions: 1. Emissions from Indonesian, African, and other fuels, Journal of Geophysical Research: Atmospheres, 108, n/a–n/a, doi:10.1029/2003JD003704, 4719, 2003.

Christian, T. J., Yokelson, R. J., Carvalho, J. A., Griffith, D. W. T., Alvarado, E. C., Santos, J. C., Neto, T. G. S., Veras, C. A. G., and Hao, W. M.: The tropical forest and fire emissions experiment: Trace gases emitted by smoldering logs and dung from deforestation and pasture fires in Brazil, Journal of Geophysical Research: Atmospheres, 112, n/a–n/a, doi:10.1029/2006JD008147, d18308, 2007.

Cofer, W. R., Winstead, E. L., Stocks, B. J., Goldammer, J. G., and Cahoon, D. R.: Crown fire emissions of CO2, CO, H2, CH4, and TNMHC from a dense Jack pine boreal forest fire, Geophysical Research Letters, 25, 3919–3922, doi:10.1029/1998GL900042, 1998.

Cogan, A., Boesch, H., Parker, R., Feng, L., Palmer, P., Blavier, J.-F., Deutscher, N. M., Macatangay, R., Notholt, J., Roehl, C., Warneke, T., and Wunch, D.: Atmospheric carbon dioxide retrieved from the Greenhouse gases Observing SATellite (GOSAT): Comparison with

ground-based TCCON observations and GEOS-Chem model calculations, Journal of Geophysical Research: Atmospheres (1984–2012), 117, doi:10.1029/2012JD018087, 2012.

Coheur, P.-F., Clarisse, L., Turquety, S., Hurtmans, D., and Clerbaux, C.: IASI measurements of reactive trace species in biomass burning plumes, Atmospheric Chemistry and Physics, 9, 5655–5667, doi:10.5194/acp-9-5655-2009, 2009.

Cressot, C., Chevallier, F., Bousquet, P., Crevoisier, C., Dlugokencky, E. J., Fortems-Cheiney, A., Frankenberg, C., Parker, R., Pison, I., Scheepmaker, R. A., Montzka, S. A., Krummel, P. B., Steele, L. P., and Langenfelds, R. L.: On the consistency between global and regional methane emissions inferred from SCIAMACHY, TANSO-FTS, IASI and surface measurements, Atmospheric Chemistry and Physics, 14, 577–592, doi:10.5194/acp-14-577-2014, 2014.

Drake, N.: Indonesia blazes threaten endangered orangutans, Nature, 527, doi:doi:10.1038/527018a, 2015.

Frankenberg, C., Meirink, J. F., Bergamaschi, P., Goede, A. P. H., Heimann, M., Körner, S., Platt, U., van Weele, M., and Wagner, T.: Satellite chartography of atmospheric methane from SCIAMACHY on board ENVISAT: Analysis of the years 2003 and 2004, Journal of Geophysical Research: Atmospheres, 111, n/a–n/a, doi:10.1029/2005JD006235, d07303, 2006.

Fraser, A., Palmer, P. I., Feng, L., Boesch, H., Cogan, A., Parker, R., Dlugokencky, E. J., Fraser, P. J., Krummel, P. B., Langenfelds, R. L., O'Doherty, S., Prinn, R. G., Steele, L. P., van der Schoot, M., and Weiss, R. F.: Estimating regional methane surface fluxes: the relative importance of surface and GOSAT mole fraction measurements, Atmospheric Chemistry and Physics, 13, 5697–5713, doi:10.5194/acp-13-5697-2013, 2013.

Fraser, A., Palmer, P. I., Feng, L., Bösch, H., Parker, R., Dlugokencky, E. J., Krummel, P. B., and Langenfelds, R. L.: Estimating regional fluxes of CO_2 and CH_4 using space-borne observations of XCH_4: XCO_2, Atmospheric Chemistry and Physics, 14, 12 883–12 895, doi:10.5194/acp-14-12883-2014, 2014.

Freeborn, P. H., Wooster, M. J., Hao, W. M., Ryan, C. A., Nordgren, B. L., Baker, S. P., and Ichoku, C.: Relationships between energy release, fuel mass loss, and trace gas and aerosol emissions during laboratory biomass fires, Journal of Geophysical Research: Atmospheres, 113, doi:10.1029/2007JD008679, 2008.

Gaveau, D. L., Salim, M. A., Hergoualc'h, K., Locatelli, B., Sloan, S., Wooster, M., Marlier, M. E., Molidena, E., Yaen, H., DeFries, R., et al.: Major atmospheric emissions from peat fires in Southeast Asia during non-drought years: evidence from the 2013 Sumatran fires, Scientific reports, 4, doi:10.1038/srep06112, 2014.

Giglio, L., Descloitres, J., Justice, C. O., and Kaufman, Y. J.: An enhanced contextual fire detection algorithm for MODIS, Remote sensing of environment, 87, 273–282, doi:10.1016/S0034-4257(03)00184-6, 2003.

Guild, L. S., Kauffman, J. B., Cohen, W. B., Hlavka, C. A., and Ward, D. E.: MODELING BIOMASS BURNING EMISSIONS FOR AMAZON FOREST AND PASTURES IN RONDÔNIA, BRAZIL, Ecological Applications, 14, 232–246, doi:10.1890/01-6009, 2004.

Hartmann, D., Klein Tank, A., Rusticucci, M., Alexander, L., Brönnimann, S., Charabi, Y., Dentener, F., Dlugokencky, E., Easterling, D., Kaplan, A., Soden, B., Thorne, P., Wild, M., and Zhai, P.: Observations: Atmosphere and Surface, book section 2, pp. 159–254, Cambridge University Press, Cambridge, United Kingdom and New York, NY, USA, doi:10.1017/CBO9781107415324.008, www.climatechange2013.org, 2013.

Huijnen, V., Wooster, M. J., Kaiser, J. W., Gaveau, D. L. A., Flemming, J., Parrington, M., Inness, A., Murdiyarso, D., Main, B., and van Weele, M.: Fire carbon emissions over maritime southeast Asia in 2015 largest since 1997, Scientific Reports, 6, 26 886, doi:10.1038/srep26886, 2016.

Hurst, D. F., Griffith, D. W., and Cook, G. D.: Trace gas emissions from biomass burning in tropical Australian savannas, Journal of Geophysical Research: Atmospheres, 99, 16 441–16 456, doi:10.1029/94JD00670, 1994.

Inness, A., Blechschmidt, A.-M., Bouarar, I., Chabrillat, S., Crepulja, M., Engelen, R. J., Eskes, H., Flemming, J., Gaudel, A., Hendrick, F., Huijnen, V., Jones, L., Kapsomenakis, J., Katragkou, E., Keppens, A., Langerock, B., de Mazière, M., Melas, D., Parrington, M., Peuch, V. H., Razinger, M., Richter, A., Schultz, M. G., Suttie, M., Thouret, V., Vrekoussis, M., Wagner, A., and Zerefos, C.: Data assimilation of satellite-retrieved ozone, carbon monoxide and nitrogen dioxide with ECMWF's Composition-IFS, Atmospheric Chemistry and Physics, 15, 5275–5303, doi:10.5194/acp-15-5275-2015, 2015.

Kaiser, J. W., Heil, A., Andreae, M. O., Benedetti, A., Chubarova, N., Jones, L., Morcrette, J.-J., Razinger, M., Schultz, M. G., Suttie, M., and van der Werf, G. R.: Biomass burning emissions estimated with a global fire assimilation system based on observed fire radiative power, Biogeosciences, 9, 527–554, doi:10.5194/bg-9-527-2012, 2012.

Kasischke, E. S. and Bruhwiler, L. P.: Emissions of carbon dioxide, carbon monoxide, and methane from boreal forest fires in 1998, Journal of Geophysical Research: Atmospheres, 107, FFR 2–1–FFR 2–14, doi:10.1029/2001JD000461, 8146, 2002.

Koppmann, R., Khedim, A., Rudolph, J., Poppe, D., Andreae, M. O., Helas, G., Welling, M., and Zenker, T.: Emissions of organic trace gases from savanna fires in southern Africa during the 1992 Southern African Fire Atmosphere Research Initiative and their impact on the formation of tropospheric ozone, Journal of Geophysical Research: Atmospheres, 102, 18 879–18 888, doi:10.1029/97JD00845, 1997.

Koppmann, R., Czapiewski, K. v., and Reid, J.: A review of biomass burning emissions, part I: gaseous emissions of carbon monoxide, methane, volatile organic compounds, and nitrogen containing compounds, Atmospheric Chemistry and Physics Discussions, 5, 10 455–10 516, doi:10.5194/acpd-5-10455-2005, 2005.

Korontzi, S., Ward, D. E., Susott, R. A., Yokelson, R. J., Justice, C. O., Hobbs, P. V., Smithwick, E. A. H., and Hao, W. M.: Seasonal variation and ecosystem dependence of emission factors for selected trace gases and PM2.5 for southern African savanna fires, Journal of Geophysical Research: Atmospheres, 108, n/a–n/a, doi:10.1029/2003JD003730, 4758, 2003.

Kuze, A., Suto, H., Nakajima, M., and Hamazaki, T.: Thermal and near infrared sensor for carbon observation Fourier-transform spectrometer on the Greenhouse Gases Observing Satellite for greenhouse gases monitoring, Applied Optics, 48, 6716–6733, doi:10.1364/AO.48.006716, 2009.

Kuze, A., suto, H., Shiomi, K., kawakami, S., Tanaka, M., Ueda, Y., Deguchi, A., Yoshida, J., Yamamoto, Y., Kataoka, F., Taylor, T. E., and Buijs, H.: Update on GOSAT TANSO-FTS performance, operations, and data products after more than six years in space, Atmospheric Measurement Techniques Discussions, 2016, 1–38, doi:10.5194/amt-2015-333, 2016.

Langner, A. and Siegert, F.: Spatiotemporal fire occurrence in Borneo over a period of 10 years, Global Change Biology, 15, 48–62, doi:10.1111/j.1365-2486.2008.01828.x, 2009.

Langner, A., Miettinen, J., and Siegert, F.: Land cover change 2002–2005 in Borneo and the role of fire derived from MODIS imagery, Global Change Biology, 13, 2329–2340, doi:10.1111/j.1365-2486.2007.01442.x, 2007.

Lee, T., Sullivan, A. P., Mack, L., Jimenez, J. L., Kreidenweis, S. M., Onasch, T. B., Worsnop, D. R., Malm, W., Wold, C. E., Hao, W. M., and Jr., J. L. C.: Chemical Smoke Marker Emissions During Flaming and Smoldering Phases of Laboratory Open Burning of Wildland Fuels, Aerosol Science and Technology, 44, i–v, doi:10.1080/02786826.2010.499884, 2010.

Liu, D., Allan, J. D., Young, D. E., Coe, H., Beddows, D., Fleming, Z. L., Flynn, M. J., Gallagher, M. W., Harrison, R. M., Lee, J., Prevot, A. S. H., Taylor, J. W., Yin, J., Williams, P. I., and Zotter, P.: Size distribution, mixing state and source apportionment of black carbon aerosol in London during wintertime, Atmospheric Chemistry and Physics, 14, 10 061–10 084, doi:10.5194/acp-14-10061-2014, 2014.

Lobert, J. M. and Warnatz, J.: Emissions from the combustion process in vegetation, in: Fire in the Environment: The Ecological, Atmospheric and Climatic Importance of Vegetation Fires,, edited by Crutzen, P. J. and Goldammer, J. G., pp. 15–37, John Wiley, 1993.

Myhre, G., Shindell, D., Bréon, F.-M., Collins, W., Fuglestvedt, J., Huang, J., Koch, D., Lamarque, J.-F., Lee, D., Mendoza, B., Nakajima, T., Robock, A., Stephens, G., Takemura, T., and Zhang, H.: Anthropogenic and Natural Radiative Forcing, in: Climate Change 2013: The Physical Science Basis. Contribution of Working Group I to the Fifth Assessment Report of the Intergovernmental Panel on Climate Change, edited by Stocker, T., Qin, D., Plattner, G.-K., Tignor, M., Allen, S., Boschung, J., Nauels, A., Xia, Y., Bex, V., and Midgley, P., chap. 8, pp. 659–740, Cambridge University Press, doi:10.1017/ CBO9781107415324.018, 2013.

O'Dell, C. W., Connor, B., Bösch, H., O'Brien, D., Frankenberg, C., Castano, R., Christi, M., Eldering, D., Fisher, B., Gunson, M., McDuffie, J., Miller, C. E., Natraj, V., Oyafuso, F., Polonsky, I., Smyth, M., Taylor, T., Toon, G. C., Wennberg, P. O., and Wunch, D.: The ACOS CO_2 retrieval algorithm Part 1: Description and validation against synthetic observations, Atmospheric Measurement Techniques, 5, 99–121, doi:10.5194/amt-5-99-2012, 2012.

O'Shea, S. J., Bauguitte, S. J.-B., Gallagher, M. W., Lowry, D., and Percival, C. J.: Development of a cavity-enhanced absorption spectrometer for airborne measurements of CH_4 and CO_2, Atmospheric Measurement Techniques, 6, 1095–1109, doi:10.5194/amt-6-1095-2013, 2013.

Othman, M. and Latif, M.: Dust and gas emissions from small-scale peat combustion, Aerosol and Air Quality Research, 13, 1045–1059, doi:10.4209/aaqr.2012.08.0214, 2013.

Page, S. E., Siegert, F., Rieley, J. O., Boehm, H.-D. V., Jaya, A., and Limin, S.: The amount of carbon released from peat and forest fires in Indonesia during 1997, Nature, 420, 61–65, doi:10.1038/nature01131, 2002.

Parker, R., Boesch, H., Cogan, A., Fraser, A., Feng, L., Palmer, P. I., Messerschmidt, J., Deutscher, N., Griffith, D. W., Notholt, J., et al.: Methane observations from the Greenhouse Gases Observing SATellite: Comparison to ground-based TCCON data and model calculations, Geophysical Research Letters, 38, doi:10.1029/2011GL047871, 2011.

Parker, R. J., Boesch, H., Byckling, K., Webb, A. J., Palmer, P. I., Feng, L., Bergamaschi, P., Chevallier, F., Notholt, J., Deutscher, N., Warneke, T., Hase, F., Sussmann, R., Kawakami, S., Kivi, R., Griffith, D. W. T., and Velazco, V.: Assessing 5 years of GOSAT Proxy XCH_4 data and associated uncertainties, Atmospheric Measurement Techniques, 8, 4785–4801, doi:10.5194/amt-8-4785-2015, 2015.

Reid, J., Koppmann, R., Eck, T., and Eleuterio, D.: A review of biomass burning emissions part II: intensive physical properties of biomass burning particles, Atmospheric Chemistry and Physics, 5, 799–825, doi:10.5194/acp-5-799-2005, 2005.

Ritung, S., Wahyunto, and Nugroho, K.: Peatland map of Indonesia, Office of Research and Development of Land Resources, Ministry of Agriculture, http://www.litbang.pertanian.go.id/unker/one/600/, 2016.

Ross, A. N., Wooster, M. J., Boesch, H., and Parker, R.: First satellite measurements of carbon dioxide and methane emission ratios in wildfire plumes, Geophysical Research Letters, 40, 4098–4102, doi:10.1002/grl.50733, 2013.

Schepers, D., Guerlet, S., Butz, A., Landgraf, J., Frankenberg, C., Hasekamp, O., Blavier, J.-F., Deutscher, N. M., Griffith, D. W. T., Hase, F., Kyro, E., Morino, I., Sherlock, V., Sussmann, R., and Aben, I.: Methane retrievals from Greenhouse Gases Observing Satellite (GOSAT) shortwave infrared measurements: Performance comparison of proxy and physics retrieval algorithms, Journal of Geophysical Research: Atmospheres (1984–2012), 117, doi:10.1029/2012JD017549, 2012.

Schroeder, W., Oliva, P., Giglio, L., and Csiszar, I. A.: The New {VIIRS} 375 m active fire detection data product: Algorithm description and initial assessment, Remote Sensing of Environment, 143, 85 – 96, doi:10.1016/j.rse.2013.12.008, 2014.

Simmonds, P., Manning, A., Derwent, R., Ciais, P., Ramonet, M., Kazan, V., and Ryall, D.: A burning question. Can recent growth rate anomalies in the greenhouse gases be attributed to large-scale biomass burning events?, Atmospheric Environment, 39, 2513 – 2517, doi:10.1016/j.atmosenv.2005.02.018, 2005.

Stockwell, C. E., Yokelson, R. J., Kreidenweis, S. M., Robinson, A. L., DeMott, P. J., Sullivan, R. C., Reardon, J., Ryan, K. C., Griffith, D. W. T., and Stevens, L.: Trace gas emissions from combustion of peat, crop residue, domestic biofuels, grasses, and other fuels: con-

figuration and Fourier transform infrared (FTIR) component of the fourth Fire Lab at Missoula Experiment (FLAME-4), Atmospheric Chemistry and Physics, 14, 9727–9754, doi:10.5194/acp-14-9727-2014, 2014.

Trenberth, K. E.: The Definition of El Niño, Bulletin of the American Meteorological Society, 78, 2771–2777, doi:10.1175/1520-0477(1997)078<2771:TDOENO>2.0.CO;2, 1997.

Trigg, S. N., Curran, L. M., and McDonald, A. K.: Utility of Landsat 7 satellite data for continued monitoring of forest cover change in protected areas in Southeast Asia, Singapore Journal of Tropical Geography, 27, 49–66, doi:10.1111/j.1467-9493.2006.00239.x, 2006.

Turner, A. J., Jacob, D. J., Wecht, K. J., Maasakkers, J. D., Lundgren, E., Andrews, A. E., Biraud, S. C., Boesch, H., Bowman, K. W., Deutscher, N. M., Dubey, M. K., Griffith, D. W. T., Hase, F., Kuze, A., Notholt, J., Ohyama, H., Parker, R., Payne, V. H., Sussmann, R., Sweeney, C., Velazco, V. A., Warneke, T., Wennberg, P. O., and Wunch, D.: Estimating global and North American methane emissions with high spatial resolution using GOSAT satellite data, Atmospheric Chemistry and Physics, 15, 7049–7069, doi:10.5194/acp-15-7049-2015, 2015.

van der Werf, G. R., Randerson, J. T., Collatz, G. J., Giglio, L., Kasibhatla, P. S., Arellano, A. F., Olsen, S. C., and Kasischke, E. S.: Continental-Scale Partitioning of Fire Emissions During the 1997 to 2001 El Niño/La Niña Period, Science, 303, 73–76, doi:10.1126/science.1090753, 2004.

van der Werf, G. R., Dempewolf, J., Trigg, S. N., Randerson, J. T., Kasibhatla, P. S., Giglio, L., Murdiyarso, D., Peters, W., Morton, D. C., Collatz, G. J., Dolman, A. J., and DeFries, R. S.: Climate regulation of fire emissions and deforestation in equatorial Asia, Proceedings of the National Academy of Sciences, 105, 20 350–20 355, doi:10.1073/pnas.0803375105, 2008.

van der Werf, G. R., Randerson, J. T., Giglio, L., Collatz, G. J., Mu, M., Kasibhatla, P. S., Morton, D. C., DeFries, R. S., Jin, Y., and van Leeuwen, T. T.: Global fire emissions and the contribution of deforestation, savanna, forest, agricultural, and peat fires (1997â€“2009), Atmospheric Chemistry and Physics, 10, 11 707–11 735, doi:10.5194/acp-10-11707-2010, 2010.

Van Leeuwen, T. and Van Der Werf, G.: Spatial and temporal variability in the ratio of trace gases emitted from biomass burning, Atmospheric Chemistry and Physics, 11, 3611–3629, doi:10.5194/acp-11-3611-2011, 2011.

Voiland, A.: Seeing Through the Smoky Pall: Observations from a Grim Indonesian Fire Season, http://earthobservatory.nasa.gov/Features/IndonesianFires, 2016.

Wang, W., Ciais, P., Nemani, R. R., Canadell, J. G., Piao, S., Sitch, S., White, M. A., Hashimoto, H., Milesi, C., and Myneni, R. B.: Variations in atmospheric CO(2) growth rates coupled with tropical temperature, Proceedings of the National Academy of Sciences of the United States of America, 110, 13 061–13 066, doi:10.1073/pnas.1219683110, 2013.

Wecht, K., Jacob, D., Sulprizio, M., Santoni, G., Wofsy, S., Parker, R., Bösch, H., and Worden, J.: Spatially resolving methane emissions in California: constraints from the CalNex aircraft campaign and from present (GOSAT, TES) and future (TROPOMI, geostationary) satellite observations, Atmospheric Chemistry and Physics Discussions, 14, 4119–4148, doi:10.5194/acp-14-8173-2014, 2014.

Wolter, K.: Multivariate ENSO Index (MEI), http://www.esrl.noaa.gov/psd/enso/mei/, 2016.

Wolter, K. and Timlin, M. S.: Measuring the strength of ENSO events: How does 1997/98 rank?, Weather, 53, 315–324, doi:10.1002/j.1477-8696.1998.tb06408.x, 1998.

Wooster, M. and Zhang, Y.: Boreal forest fires burn less intensely in Russia than in North America, Geophysical Research Letters, 31, doi:10.1029/2004GL020805, 2004.

Wooster, M., Freeborn, P., Archibald, S., Oppenheimer, C., Roberts, G., Smith, T., Govender, N., Burton, M., and Palumbo, I.: Field determination of biomass burning emission ratios and factors via open-path FTIR spectroscopy and fire radiative power assessment:

headfire, backfire and residual smouldering combustion in African savannahs, Atmospheric Chemistry and Physics, 11, 11 591–11 615, doi:10.5194/acp-11-11591-2011, 2011.

Wooster, M., Perry, G., and Zoumas, A.: Fire, drought and El Niño relationships on Borneo (Southeast Asia) in the pre-MODIS era (1980–2000), Biogeosciences, 9, 317–340, doi:10.5194/bg-9-317-2012, 2012.

Wooster, M. J., Ceccato, P., and Flasse, S. P.: Cover - Indonesian fires observed using AVHRR, International Journal of Remote Sensing, 19, 383–386, doi:10.1080/014311698216035, 1998.

Wooster, M. J., Roberts, G., Perry, G. L. W., and Kaufman, Y. J.: Retrieval of biomass combustion rates and totals from fire radiative power observations: FRP derivation and calibration relationships between biomass consumption and fire radiative energy release, Journal of Geophysical Research: Atmospheres, 110, doi:10.1029/2005JD006318, d24311, 2005.

Yokelson, R. J., Griffith, D. W. T., and Ward, D. E.: Open-path Fourier transform infrared studies of large-scale laboratory biomass fires, Journal of Geophysical Research: Atmospheres, 101, 21 067–21 080, doi:10.1029/96JD01800, 1996.

Yokelson, R. J., Goode, J. G., Ward, D. E., Susott, R. A., Babbitt, R. E., Wade, D. D., Bertschi, I., Griffith, D. W., and Hao, W. M.: Emissions of formaldehyde, acetic acid, methanol, and other trace gases from biomass fires in North Carolina measured by airborne Fourier transform infrared spectroscopy, Journal of Geophysical Research: Atmospheres, 104, 30 109–30 125, doi:10.1029/1999JD900817, 1999.

Yokelson, R. J., Christian, T. J., Karl, T., and Guenther, A.: The tropical forest and fire emissions experiment: laboratory fire measurements and synthesis of campaign data, Atmospheric Chemistry and Physics, 8, 3509–3527, doi:10.5194/acp-8-3509-2008, 2008.

Yokelson, R. J., Andreae, M. O., and Akagi, S.: Pitfalls with the use of enhancement ratios or normalized excess mixing ratios measured in plumes to characterize pollution sources and aging, Atmospheric Measurement Techniques, 6, 2155, doi:10.5194/amt-6-2155-2013, 2013.

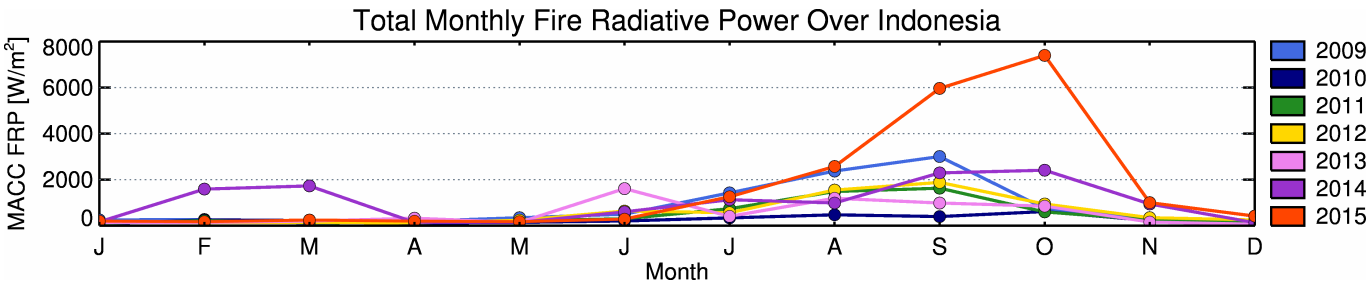

Figure 1. Time series of the monthly total Fire Radiative Power density (W/m^2) recorded over the Indonesian region (defined as 5°N-10°S, 90°E-150°E) between 2009 and 2015, calculated using data from the Copernicus Atmosphere Monitoring Services (CAMS') Global Fire Assimilation System (Kaiser et al., 2012). September and October 2015 are clearly anomalous compared to the previous years shown, highlighting the effect of this year's El Niño on the regions fire activity.

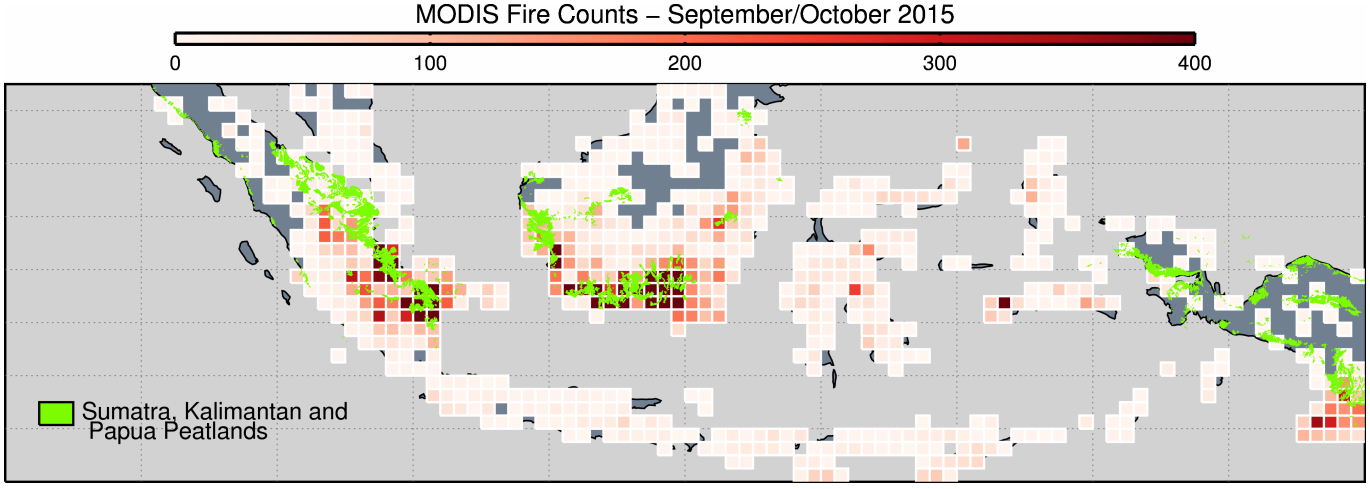

Figure 2. MODIS fire counts for September/October 2015 over the Indonesia, gridded into 0.5°x0.5° boxes. Also overlaid are the locations of known peatlands in Sumatra (left), Kalimantan (centre) and Papua (right).

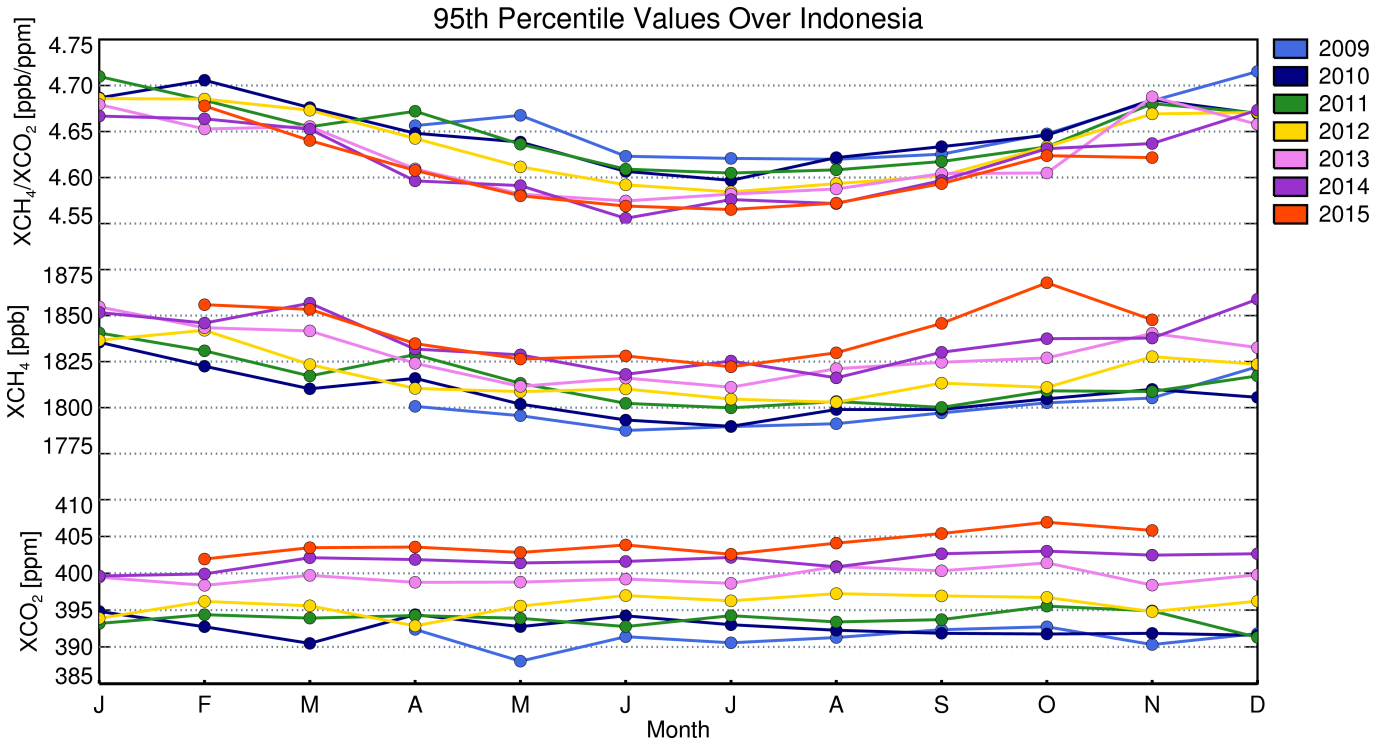

Figure 3. Timeseries showing the monthly 95th-percentile values over Indonesia for the GOSAT Proxy XCH_4/XCO_2 (top) as well as the individual XCH_4 (middle) and XCO_2 (bottom) components of the Proxy data for the entire GOSAT data record (2009-present).

Table 1. Table showing the mean and standard deviation over Indonesia in September/October 2015 of the XCH_4/XCO_2 Ratio (left), the retrieved XCO_2 (centre) and the retrieved XCH_4 (right) for all data~~(green)~~, data determined to be unaffected by fire ~~(blue)~~ and data determined to be affected by fire~~(red)~~.

	XCH_4/XCO_2 (ppb/ppm)		XCO_2 (ppm)		XCH_4 (ppb)	
	Mean	Std. Dev	Mean	Std. Dev	Mean	Std. Dev
All	4.54	0.033	399.9	4.88	1814.4	25.14
Clear	4.52	0.023	399.9	4.02	1805.5	18.43
Fire-affected	4.59	0.035	401.1	7.54	1840.1	37.83

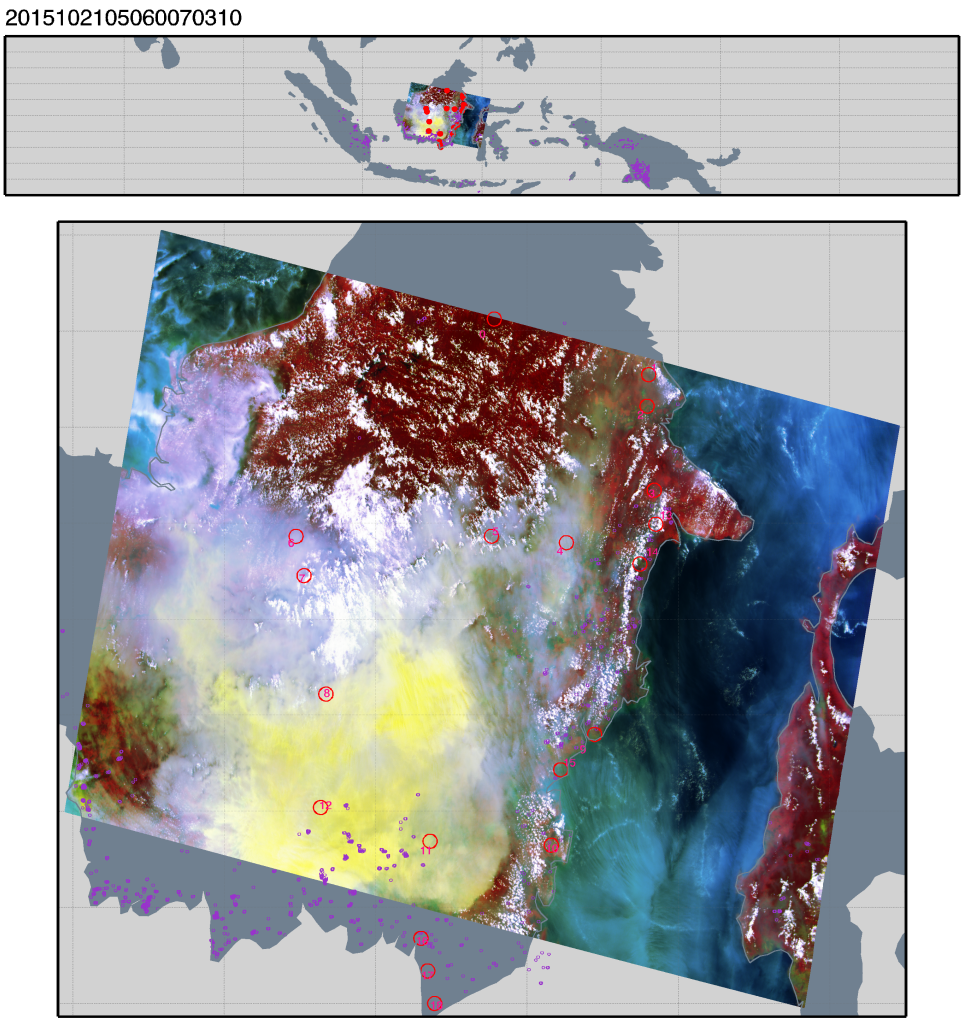

Figure 4. False-colour image (RGB = CAI Band 3, 2, 1) derived from data taken by the GOSAT Cloud and Aerosol Imager, collected when the GOSAT satellite passed over the island of Borneo on 21st October 2015 (around 1pm local time, 5am UTC), a period when extreme fires were burning across much of Central Kalimantan. GOSAT TANSO-FTS sounding locations are identified by the numbered large red circles, with the MODIS active fire detections identified by the small purple circles.

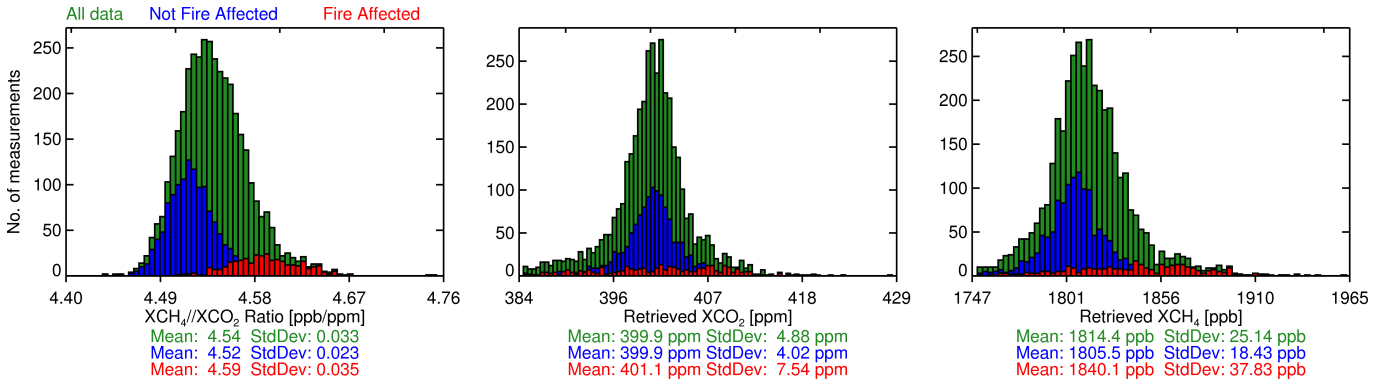

Figure 5. Histograms showing the distributions over Indonesia in September/October 2015 of the XCH_4/XCO_2 Ratio (left), the retrieved XCO_2 (centre) and the retrieved XCH_4 (right) for all data (green), data determined to be definitely fire-affected by fire emissions (red), and that classed as "clear" (blue). Also included are the corresponding mean and stdev values for each distribution.

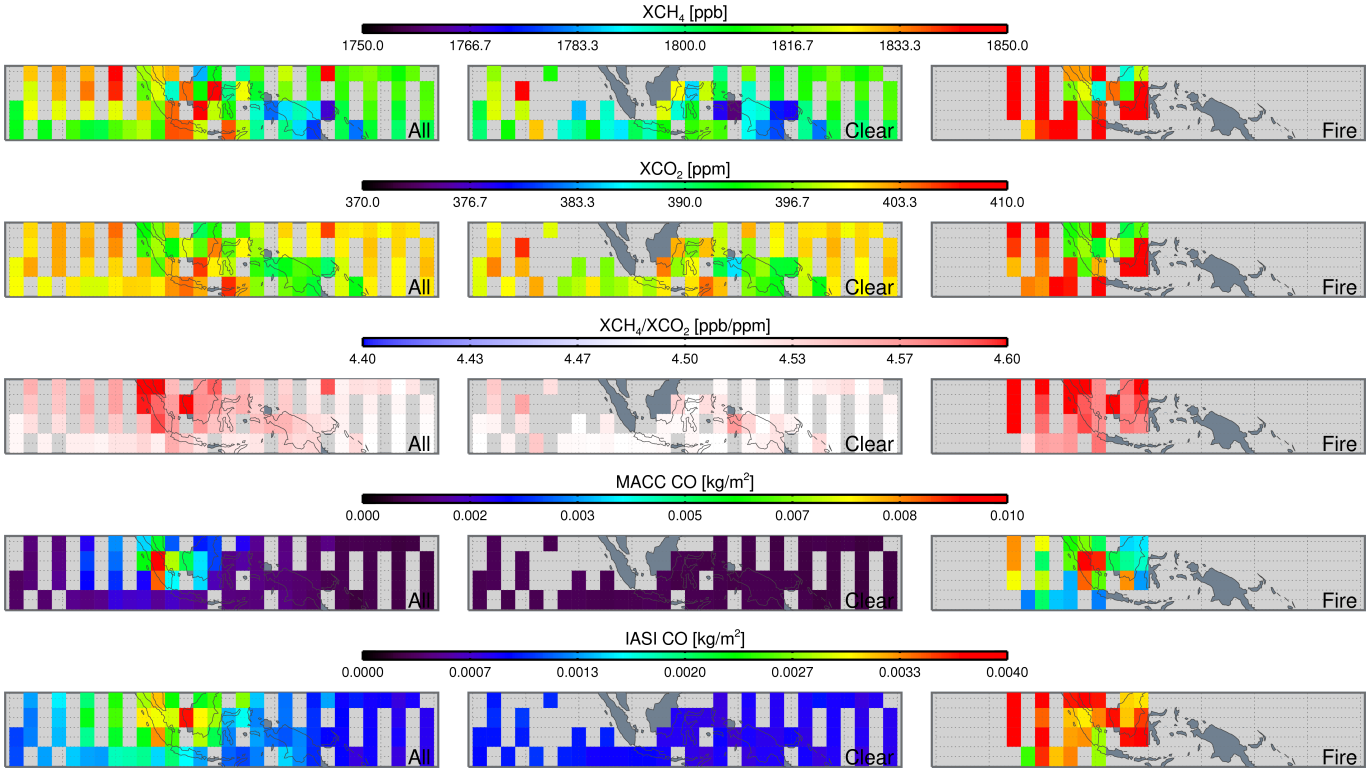

Figure 6. Indonesia trace gas distributions for September-October 2015 showing (top to bottom): the GOSAT-retrieved XCH_4, XCO_2, and XCH_4/XCO_2 ratio, along with the CAMS carbon monoxide (CO) total column and the measured IASI CO total column. The left column shows all data gridded at 2° x2° degrees , the central column shows only those points determined to be "clear" using the criteria of Section 4, and the right column shows the data determined to be fire affected based on the same criteria.

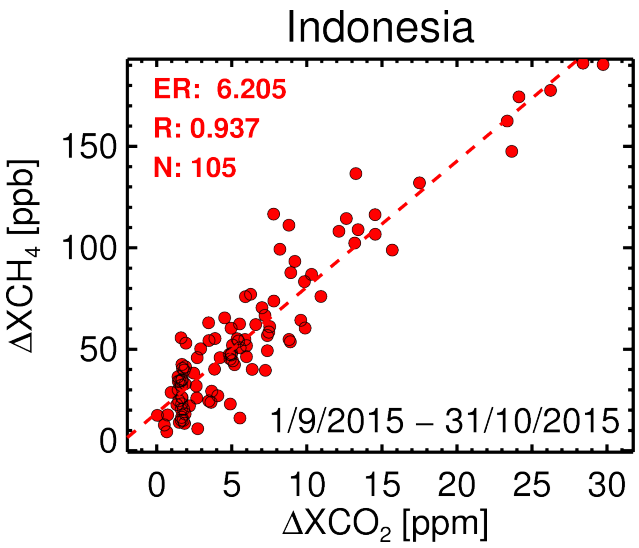

Figure 7. Scatterplot of GOSAT-derived ΔXCH_4 vs ΔXCO_2 values for large-scale fire plumes seen over ~~Indonesia~~ Indonesian region (of the type seen in Figure 4) from 1st September ~~region from 1st September~~ 2015 to 31st October 2015, calculated as the total column difference between the 'fire affected' and corresponding clear 'background' TANSO-FTS soundings. The CH_4/CO_2 emission ratio, ER (ppb/ppm), is calculated from the gradient of a linear best fit, shown as the dashed line. Also shown are the correlation coefficient, R and the number of soundings, N.

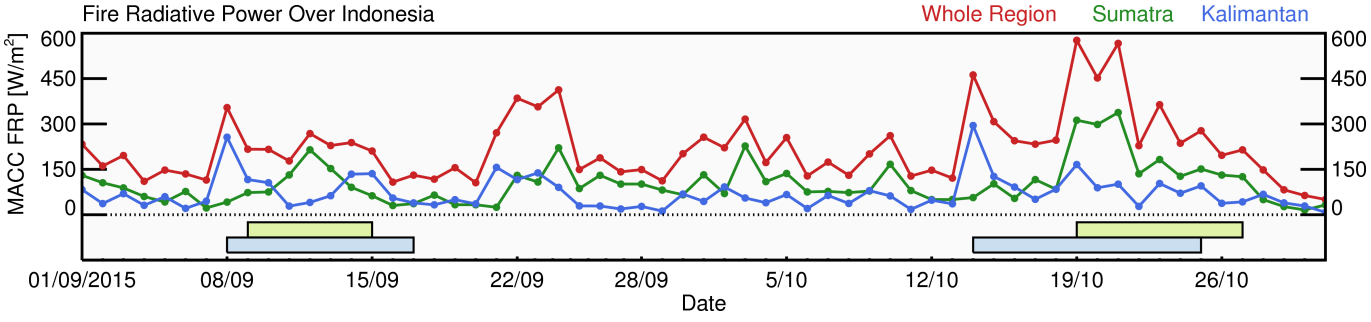

Figure 8. Daily Fire Radiative Power density (red line) taken from the Global Fire Assimilation System (GFAS) (Kaiser et al., 2012), operated as part of the Copernicus Atmosphere Service (CAMS). Data are shown from 1st September to 31st October 2015, for both the entire Indonesian landmass (red) and separately for the regions of Sumatra and Kalimantan. Two specific time periods are highlighted (referred to as Period 1 and Period 2), Period 1 covering 9th-15th September (Sumatra) and 8th-17th September (Kalimantan), and Period 2 covering 19th-27th October (Sumatra) and 14th-25th October (Kalimantan)

.

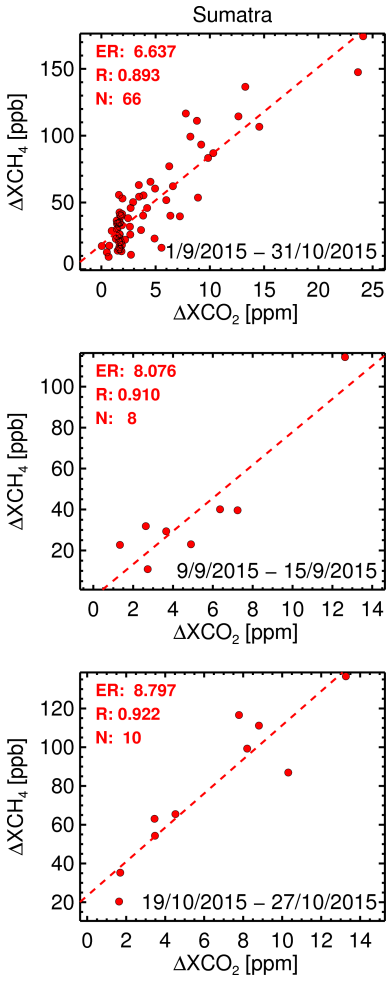

Figure 9. Scatterplots of ΔXCH_4 vs ΔXCO_2 derived for Sumatran large-scale fire plumes via analysis of TANSO-FTS data for the time periods detailed in Fig. 8: Sept-Oct 2015 (top), Period 1: 9th-15th September (middle), and Period 2: 19th-27th October (bottom). The CH_4/CO_2 emission ratio is calculated as the gradient of a linear fit to the data (dashed line). The correlation coefficient R and the number of soundings N are also shown.

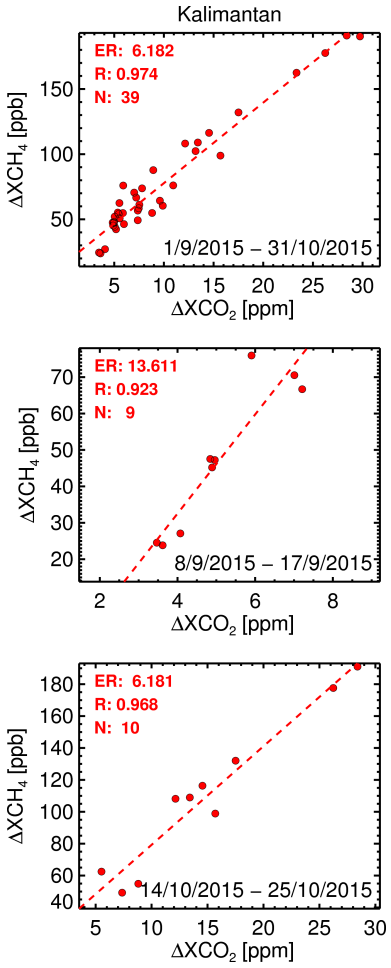

Figure 10. Scatterplots of ΔXCH_4 vs ΔXCO_2 derived for Kalimantan large-scale fire plumes via analysis of TANSO-FTS data for the time periods detailed in Fig. 8: Sept-Oct 2015 (top), Period 1: 8th-17th September (middle), and Period 2: 14th-25th October (bottom). The CH_4/CO_2 emission ratio is calculated as the gradient of a linear fit to the data (dashed line).The correlation coefficient R and the number of soundings N are also shown.

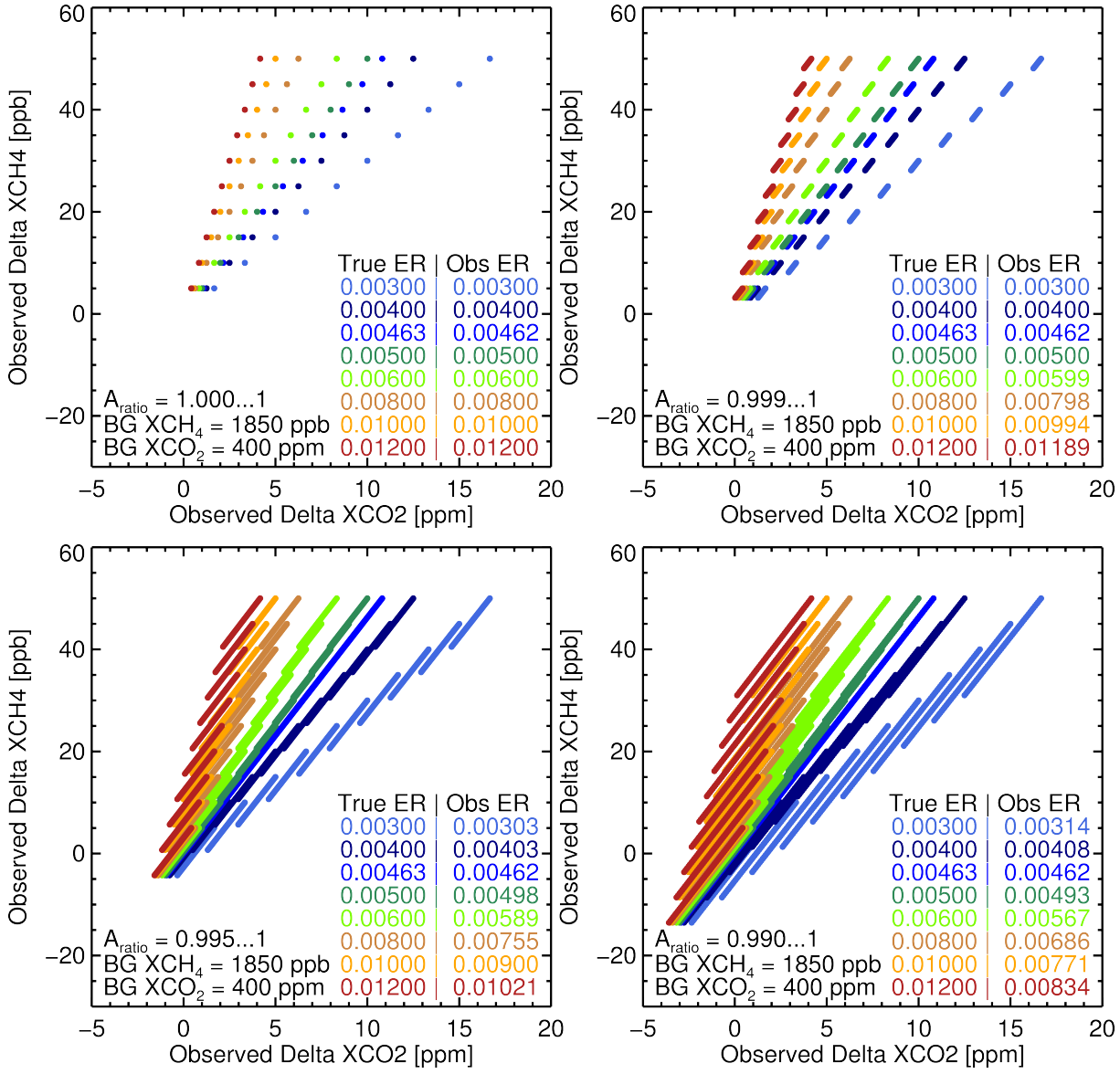

Figure 11. Implementation of Equation ~~X~~ A13 with ΔXCH_4 varied between 5-50 ppb for ERs ranging from 0.003 to 0.009 for different ranges of A_{ratio}. The true emission ratios and the emission ratios derived from the observed correlation are shown in each panel. The top left figure shows a fixed value of A_{ratio} = 1 while the remaining panels (clockwise) show the value of A_{ratio} ranging from 0.999 to 1, 0.99 to 1 and 0.995 to 1.

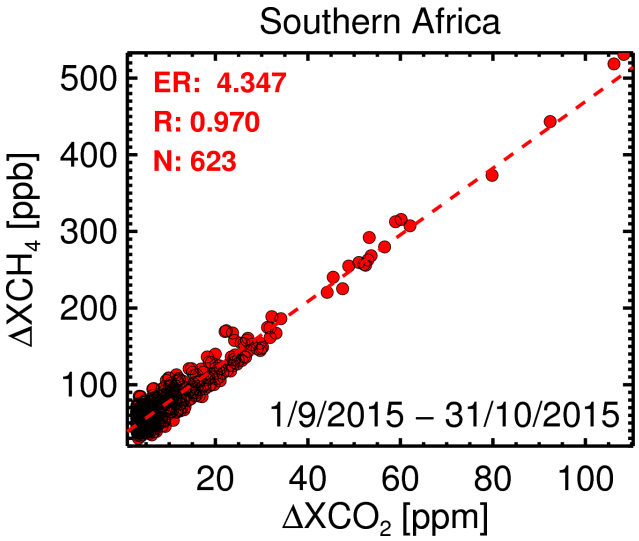

Figure 12. Scatterplot showing the ΔXCH_4 vs ΔXCO_2 values, calculated as the difference between the values in the fire-affected soundings to those in the background cases over the entire southern African region for 1st September 2015 to 31st October 2015. The CH_4/CO_2 emission ratio is calculated from the gradient of the linear best fit, which is shown along with the correlation coefficient R and the number of sounding pairs N. This GOSAT-derived ER is very similar to the 'fire averaged' CH_4 to CO_2 ER of 4.3 $\pm$ 1.7 ppb/ppm derived by Wooster et al. (2011) using open path FTIR spectroscopy measurements close to source on these type of savannah fire events. ~~This line of best fit is also shown, along with the correlation coefficient, R and the number of sounding, N.~~

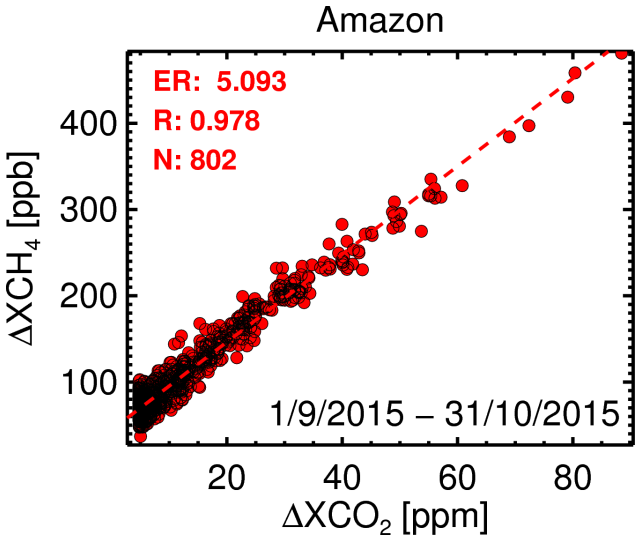

Figure 13. Scatterplot showing the ΔXCH_4 vs ΔXCO_2 values, calculated as the difference between the values in the fire-affected soundings to those in the background cases over the entire Amazonian region for 1st September 2015 to 31st October 2015. The CH_4/CO_2 emission ratio is calculated from the gradient of a linear fit to the data. This line of best fit is also shown, along with the correlation coefficient, R and the number of soundings, N.